HHS Public Access

Author manuscript

Wiley Interdiscip Rev Nanomed Nanobiotechnol. Author manuscript; available in PMC 2020 September 01.

Published in final edited form as:

Wiley Interdiscip Rev Nanomed Nanobiotechnol. 2019 September ; 11(5): e1560. doi:10.1002/wnan.1560.

Recent Advances in Photodynamic Therapy for Cancer and Infectious Diseases

Xutong Shi,
Washington State University, xutong.shi@wsu.edu

Can Yang Zhang*,
Washington State University, canyang.zhang@wsu.edu

Jin Gao,
Washington State University, jin.gao3@wsu.edu

Zhenjia Wang*
Washington State University, zhenjia.wang@wsu.edu

Abstract

Photodynamic therapy (PDT) is a treatment by combining light and a photosensitizer to generate ROS for cellular damage, and is used to treat cancer and infectious diseases. In this review, we focus on recent advances in design of new photosensitizers for increased production of ROS and in genetic engineering of biological photosensitizers to study cellular signalling pathways. A new concept has been proposed that PDT-induced acute inflammation can mediate neutrophil infiltration to deliver therapeutics in deep tumour tissues. Combination of PDT and immunotherapies (neutrophil-mediated therapeutic delivery) has shown the promising translation of PDT for cancer therapies. Furthermore, a new area in PDT is to treat bacterial infections to overcome the antimicrobial resistance. Finally, we have discussed the new directions of PDT for therapies of cancer and infectious diseases. In summary, we believe that rational design and innovations in nanomaterials may have a great impact on translation of PDT in cancer and infectious diseases.

Keywords

PDT; Photosensitizers; Nanoparticles; Cancer Therapy; Antimicrobial Therapy and Antibiotic Resistance

1 INTRODUCTION

Photodynamic therapy (PDT) is a treatment that combines special drugs, so-called photosensitizing agents with light to destroy cancer cells to treat cancers (Castano, Mroz, & Hamblin, 2006; Fan, Huang, & Chen, 2016) or kill microorganisms for management of

*Corresponding authors: Can Yang Zhang and Zhenjia Wang, Washington State University, zhenjia.wang@wsu.edu.

Conflict of Interest

The authors declare no conflict of interest.

infectious diseases (Wainwright et al., 2017). The drugs only work when they are activated by certain energy of light. PDT may also be named by photoradiation therapy, phototherapy or photochemical therapy.

Figure 1 shows a process of PDT. Upon exposure to a light with an appropriate wavelength, a photosensitizer (PS) is excited from a ground state to an excited state. Prior to going back to the ground state, the excited PS may transfer energy directly to surrounded tissue oxygen to produce reactive oxygen species (ROS), such as singlet oxygen ($^1O_2$), superoxide anions ($O_2^{\cdot -}$) and hydroxyl radicals ($OH^{\cdot}$) (D. E. Dolmans, D. Fukumura, & R. K. Jain, 2003). Amidst these ROS, $^1O_2$ is a primary toxic photochemical product that directly or indirectly destroys tumor cells via apoptotic, necrotic and autophagy-associated cell death (Abbas, Zou, Li, & Yan, 2017; Abrahamse & Hamblin, 2016; Fan et al., 2016; Triesscheijn, Baas, Schellens, & Stewart, 2006). The photosensitizing agent is either administered via intravenous or local injections depending on disease models. In addition, PDT usually requires oxygen existing in tumor tissues to produce ROS for tumor damage. The recent advances in material engineering allow PDT to be operated in hypoxic environments (low oxygen) (M. Derosa & J Crutchley, 2002; Fan et al., 2016).

PDT is increasingly recognized as an emerging clinical tool in cancer therapy besides other therapies (such as surgery and radiation therapy) because there are several advantages, such as tumor targeting, minimal invasiveness, reduced systemic cytotoxicity, low cost and spatiotemporal control of light exposed to tumors (Dang, He, Chen, & Yin, 2017). PDT is involved with three components: non-toxic PSs, light and tissue oxygen. In general, two major steps in PDT include delivery of PSs into patients, and then irradiation of tumor tissues with a light at a specific wavelength to activate PSs (P. Agostinis et al., 2011). There are several photosensitizing agents currently approved by the US Food and Drug Administration (FDA) to treat certain cancers. For example, Porfimer sodium (Photofrin) is used to treat esophagus cancer and non-small cell lung cancer (Simone et al., 2012; Yano, Hatogai, Morimoto, Yoda, & Kaneko, 2014).

Infectious diseases are host disorders caused by microorganisms, such as bacteria, viruses, fungi or parasites. In particular, bacterial infections are the globe threat due to the exponentially increased resistance to antibiotics. The studies in 2015 show that there would have been 300 million deaths for the costs of $100 trillion by 2050 if we do not have developed new agents to control the growth of multi-drug resistance to bacteria (Kashef, Huang, & Hamblin, 2017). To overcome antibiotic resistance, several strategies have been developed. For example, outer membrane vesicles derived from bacteria were used as vaccines to prevent bacterial infections (S. Wang, Gao, & Wang, 2018). Recent advances in nanotechnology allow to develop a facile method to generate a vaccine from the whole bacterial membrane nanovesicles using nitrogen cavitation. This new platform of vaccines may rapidly respond to the epidemic of bacterial infections (S. Wang, Gao, Li, Wang, & Wang, 2018). Except prophylactic therapy to bacterial infections, it is needed to find promising non-toxic and non-invasive antimicrobial strategies that can treat effectively and quickly compared to current antibiotic methods without development of bacterial resistance. The promising substitute is called antimicrobial photodynamic inactivation (aPDI)

(Wainwright et al., 2017), but the central concept of aPDI is similar to PDT where a photosensitizing agent can mediate the death of bacteria by light.

In this review, we are focused on addressing the challenges of PDT in cancer and infectious diseases, and how nanomaterial design and nanotechnology overcome these challenges. There are two main sections: 1) In cancer therapies, we will discuss new nanomaterials developed to increase ROS generation to improve PDT for cancer; 2) In therapy to infectious diseases, we will describe the concept of aPDI and discuss the new opportunities of aPDI to overcome antibiotic resistance in antimicrobial therapy.

2 PDT IN CANCER THERAPY

2.1 Challenges in Cancer Therapies

While PDT has been used in the past decades, translation of PDT in clinical settings is slow. PDT is still an alternative or supporting treatment in cancer therapies due to several issues (Dougherty, Grindey, Fiel, Weishaupt, & Boyle, 1975). PDT can only treat cancers where light can reach. For example, it is usually used to treat skin cancer. In addition, PDT cannot be used to treat metastatic tumors and treat patients with blood diseases or allergy to PSs. Furthermore, although PDT looks like a simple means to treat cancer, it can be still challenging to proper operations in PDT because PDT includes several technologies, such as lasers and applicators required for comprehensive training (Patrizia Agostinis et al., 2011). In terms of basic research on PDT, a major issue for translation of PDT is to develop novel approaches to specifically deliver PSs in tumor sites and generate high levels of ROS (Zijian Zhou, Jibin Song, Liming Nie, & Xiaoyuan Chen, 2016). Understanding the immunology in tumor microenvironments is important to develop combination therapies of PDT and immunotherapy (Konan-Kouakou, Boch, Gurny, & Allemann, 2005). Recent studies have demonstrated some interesting approaches used to overcome the issues in PDT (Durantini, Greene, Lincoln, Martinez, & Cosa, 2016; Starkey et al., 2008; C. Zhang et al., 2016). With the advances in nanotechnology (H. Chen et al., 2015; Torchilin, 2014; Z. Wang, Li, Cho, & Malik, 2014; Z. Wang, Tiruppathi, Cho, Minshall, & Malik, 2011; Z. Wang, Tiruppathi, Minshall, & Malik, 2009), new nanomaterials and formulations have been designed and prepared to improve PDT.

While several reviews have reported the progress in PDT (Abbas et al., 2017; Dang et al., 2017; Fan et al., 2016; Vankayala & Hwang, 2018; Z. Zhou, J. Song, L. Nie, & X. Chen, 2016), developments of PDT are dramatic in recent years in new material design and new concepts to improve the performance of PDT. Therefore, it may be necessary to review the current status of PDT in cancer therapy and to discuss the future directions. The focus of this section is to discuss several new technologies to increase ROS generation, advanced nanomaterials (such as conjugated polymers) and generation of ROS using genetic engineering. In addition, we will introduce a new concept of aggregation-induced emission (AIE) used in PDT. Tumor microenvironments are complicated and are involved with infiltration of immune cells. A new idea was proposed that PDT can be utilized to prime tumor tissues to activate neutrophil infiltration in tumors, thus nanotherapeutics can hijack neutrophils to increase drug delivery into tumor tissues (Dong, Chu, & Wang, 2017, 2018). Based on this concept, the combination of PDT and immunotherapy was proposed to treat

cancer. The recent advances in PDT demonstrate the potential of translation in combinatory therapies.

Three topics will be discussed: 1) Increased ROS production in tumors via design of novel nanomaterials; 2) Developments on targeting of photosensitizers via genetical bioengineering and biofunctionalization; 3) New concepts and technologies in combination of PDT and immunotherapies. Finally, we will discuss the perspectives in translational opportunities of PDT.

2.2 Increased ROS production in PDT

A PS in PDT is a central component in generating ROS, thus the rational design of PSs is critical to improve PDT efficacy. With the advances in nanotechnologies and new materials, several new nanomaterials and concepts have been developed to construct new PSs. We will discuss several new materials to generate ROS, such as conjugated polymer nanoparticles and donor-acceptor pairs.

2.2.1 Regulating ROS generation using novel nanoparticles—Conjugated polymers have been used in electronic devices and fluorescent materials (Z. Wang & Rothberg, 2007; Y. Zhang, Wang, Ng, & Rothberg, 2007). Recent studies have shown that conjugated polymers form nanoparticles for diagnostics, bioimaging and cancer therapies. For example, conjugated polymer-based nanotheranostic systems were constructed for PDT used in cancer therapies, but their ROS generation was not sufficient, thus potentially limiting their therapeutic outcomes. Recent studies are focused on improving PDT efficacy *via* controlling the generation of ROS (Zou, Chang, Li, & Wang, 2017).

Zhu *et al.* proposed a hybrid approach to regulate PDT for optimized cancer therapy using semiconducting polymer nanoparticles (SPNs) (Zhu et al., 2017). There are two major components in the nanotheranostics: nanoceria (cerium oxide nanoparticle) and PCPDTBT (poly(cyclopentadithiophene-*alt*-benzothiadiazole) (Figure 2A). Nanoceria acts as a ROS regulator and PCPDTBT serves as a NIR PS. Nanoceria can scavenge ROS at physiological pH 7.4 and increase ROS generation at the acidic environment due to the switchable reduction-oxidation states of Ce^{3+} and Ce^{4+} in nanoparticles (Figure 2B). SPNs were prepared with the different amounts of nanoceria in order to compare the doping effect of nanoceria (SPN-0 is 0 w/w% of nanoceria, SPN-C23 is 23 w/w% of nanoceria). To study the ROS scavenging ability of SPNs, 2',7'-dichlorofluorescin diacetate (H_2DCFDA) was used as a ROS indicator to measure the production of ROS in the solution of SPNs, because non-fluorescent H_2DCFDA can be oxidized to highly-fluorescent DCF when ROS exist. The results showed that at the neutral pH 7.4, ROS generation was inhibited by SPN-C23 compared to control groups (SPN-0 or without SPNs) (Figure 2C). Subsequently, production of ROS at both neutral (pH=7.4) and acidic (pH=6.5) conditions was measured by H_2DCFDA after laser irradiation at an NIR wavelength of 808 nm. The results in Figure 2D and E showed that the fluorescence intensity of ROS indicator in both SPN-0 and SPN-C23 groups increased proportionally with the irradiation time in 5 minutes, indicating the rapid production of ROS. Nevertheless, it is interesting to observe a remarkable difference in ROS production at pH = 7.4 from at pH = 6.5 in the presence of SPN-C23, showing that SPNs

doped with higher level of nanoceria had the different features of ROS generation and it was dependent on tissue microenvironments. Furthermore, *in vivo* experiments were conducted using the xenograft 4T1 tumor mouse model. In PDT, the tumor growth was efficiently suppressed in both SPN-C23 and SPN-0 groups, however, SPN-C23 showed the stronger capability to inhibit tumor growth compared to SPN-0 due to the higher level of ROS production in the acidic tumor microenvironment (Figure 2F). To address whether nanoceria-doped SPNs caused the damage to healthy tissues during PDT, healthy mice were administered by SPN-0 and SPN-C23 respectively and subsequently they were irradiated with NIR light. The histological analysis demonstrated that SPN-C23 maintained the intact structures of mouse muscles compared to SPN-0 administered in mice (Figure 2G). This study demonstrates that the rational design of SPN doped with nanoceria is important to simultaneously kill tumor cells and protect healthy tissues when ROS production is dependent tissue microenvironments.

Liu *et al.* designed copper ferrite nanospheres (CFNs) to regulate tumor microenvironments and to increase ROS generation in PDT (Liu et al., 2018). They took advantage of the Fenton reaction and integrated with PDT to create ROS-mediated nanotherapeutics for improving antitumor efficacy. The relatively high concentration of H_2O_2 leads to generation of toxic ROS (·OH) restricted only in tumor microenvironments, thus protecting healthy tissues from the damage. CFNs have two redox pairs (Fe^{2+}/Fe^{3+} and Cu^{+}/Cu^{2+}), which enable them to produce more efficient ·OH through Fenton reactions after illuminated with 650 nm laser. Moreover, CFNs can regulate the tumor microenvironment to manage tumor hypoxia and antioxidation through a Fenton reaction by catalyzing H_2O_2 to generate O_2 and depletion of glutathione (GSH) by Fe^{3+} and Cu^{2+}. Therefore, this approach offers effective PDT (Figure 3A).

Besides, Noh *et al.* proposed a mitochondrial targeting and brominated photodynamic therapeutic agent (MitDt) (Noh et al., 2018). Mitochondria are crucial organelles in mammalian cells and their functions are closely related to cell metabolism and signal transduction (Wallace, 2012; X. Wang, Peralta, & Moraes, 2013). Targeting mitochondria by cationic agents enhances the accumulation and retention of agents in tumor cells due to the negatively charged transmembrane potential of mitochondria, therefore, avoiding damage to healthy cells (Chandel, 2014). The heavy atom substitution into the PS enables the high ROS production compared to the original dye due to low energy loss in excited states. Hence, integrating a brominated PDT agent (heptamethine cyanine dye) with the cationic mitochondrial targeting agent (triphenylphosphonium derivative) can lead to effective ablation to tumor cells. Moreover, in order to obtain the charge balance and solubility of therapeutic agents, the N-alkyl side chain was modified. This study has demonstrated enhanced cancer therapies (Figure 3B).

2.2.2 Boosting singlet oxygen generation using a donor-acceptor system—

The limited toxic $^1O_2$ production and low photon utilization of PSs hinder the PDT applications even though NIR is used. To address this problem, Huang *et al.* proposed a novel strategy to create a dyad PS based on a resonance-energy-transfer (RET) mechanism. This new formulation was able to dramatically enhance NIR light absorption efficiency and amplify $^1O_2$ production because lower dosage of PSs and power of the NIR light were

required (L. Huang et al., 2017). Herein, the donor of fluorophore moiety B-1 (distyryl-BODIPY) was attached to the acceptor of PS moiety B-2 (diiodo-distyryl-BODIPY) to form a dyad molecule (RET-BDP) (Figure 4A) (He, Lo, Yeung, Fong, & Ng, 2011). With this combination, RET-BDP showed the superior toxic $^1O_2$ production after irradiated with low-power NIR LED light compared to the PS B-2 alone. To generate water soluble and tumor targetable nanoparticles, RET-BDP was encapsulated with F-127-folic acid (RET-BDP-TNM). Upon irradiation by NIR LED light (10mW cm^{-2}), RET-BDP-TNM demonstrated the better PDT effect in *in vitro* and *in vivo* experiments compared to unmodified PSs. In Figure 4B, RET-BDP shows an increased absorption band peak compared to B-1 and B-2 alone. The fluorescence emission spectra indicated that the donor B-1 had an emission peak at 670 nm alone, while conjugated to B2, in RET-BDP, the emission of the donor B-1 was suppressed largely, proving that efficient energy transfer existed (Figure 4C). After encapsulated by F-127-folic acid, the small-size nanoparticle (12 ± 3 nm) RET-BDP-TNM was prepared. In controls, B1-TNM and B2-TNM were also prepared by encapsulation of B-1 and B-2 using F-127-FA, respectively. The $^1O_2$ production of RET-BDP-TNM was measured with 1,3-diphenylisobenzofuran (DPBF). RET-BDP-TNM displayed quick and improved $^1O_2$ production under the irradiation of NIR LED light with respect to that of B1-TNM or B2-TNM alone (Figure 4D). Afterwards, they took advantage of propidium iodide (PI) assay to evaluate PDT effect of RET-BDP-TNM in HeLa cells. Figure 4E clearly shows that the PI stained dead cells were observed after irradiation with NIR light, and the cell viability was increased in the presence of sodium azide to scavenge $^1O_2$, implying that the cell death was associated with ROS. 2’7’-dichlorofluorescin diacetate (DCFH-DA) was utilized to test the ROS production of RET-BDP-TNM in HeLa cells. Figure 4F obviously displays substantial generation of ROS of RET-BDP-TNM in tumor cells irradiated with NIR light (bright green dots), and the emission of DCFH-DA was decreased in the presence of sodium azide, suggesting ROS were scavenged. These results support that RET-BDP-TNM effectively produces $^1O_2$ to enhance cancer therapy (Figure 4G).

Tumors form a unique microenvironment, and it is challenging that PDT treatment can completely eradicate tumors. Therefore, it is required to develop synergistic methods combined with PDT (Zhou et al., 2014; Zuluaga & Lange, 2008). The combination of PDT with other therapeutic methods may take the full advantages of each module, thus producing much stronger anticancer effects than individual therapy (i.e. “1+1>2”). Unlike PDT, ideal photothermal therapy (PTT) does not require oxygen in tumor microenvironment. Owing to this characteristic, PTT is a phototherapy with a great potential in tumor ablation that uses the heat generated from biocompatible photothermal agents accumulated in tumors to kill tumor cells without damaging healthy tissue (Q. Chen et al., 2016; Du, Qin, Ma, Zhang, & Xing, 2017; J. Zhang et al., 2017; S. Zhang et al., 2017). Nonetheless, PTT alone is not enough to eradicate tumor cells due to the rapid development of resistance to thermal stress of cancer cells, hence limited therapeutic efficacy was observed (Feder & Hofmann, 1999; Linlin et al., 2016). Considering this, PTT combined with PDT can serve as a very promising strategy to increase the cancer treatment efficacy (Bhana et al., 2016; Kerong et al., 2015; Lin et al., 2013; Xing et al., 2016; Yan, Bjornmalm, & Caruso, 2013). Yang *et al.* proposed a donor-acceptor (D-A) conjugated-polymer nanoparticles (CP-NPs) used for dual PDT/PTT treatment (Figure 5A) (Tao et al., 2017). The D-A-type CP (BIBDF-BT) was

synthesized by alkyl-chain-grafted bithiophene (BT) segment as an electron donor and (3E, 7E)-3,7-bis (2-oxoindolin-3-ylidene)benzo-[1,2-b:4,5-b']-difuran-2,6(3H,7H)-dione (BIBDF) unit as an isoindigo-based electron acceptor. Subsequently, D-A-type CP-NPs were formed by encapsulating in poly(ethylene glycol)$_{114}$-b-poly(caprolactone)$_{60}$ (PEG-PCL). The energy coupling of BT and BIBDF forms a low band gap, thus shifting absorption to NIR. The energy transfer in the excited donor-acceptor system induced singlet-to-triplet transition and generated ROS. In addition, the high electron-deficiency of isoindigo derivative led to the efficient nonradiative decay and produced heat (Figure 5B). The simultaneous generation of ROS and heat at tumor sites promoted the tumor ablation in synergistic PDT/PTT treatment (Tao et al., 2017). Figure 5C showed that CP-NPs exhibited a good photostability after repeatable irradiation and cooling processes since CP-NPs displayed the negligible change in their temperature elevation as compared to gold nanorods (AuNRs) and ICG (Indocyanine green)-loaded PEG-PCL micelles (ICG-M). Further studies showed that CP-NPs had a good ability to continuously produce $^1O_2$ during 15 min irradiation (Figure 5D). In 4T1 tumor cells, it is found that CP-NPs were able to produce remarkable intracellular $^1O_2$ under irradiation at a low concentration of 0.5 μg mL^{-1} CP (Figure 5E). Subsequently, they evaluated *in vivo* ability of generating ROS and hyperthermia in tumor-bearing mice administered with CP-NPs, followed by exposing the tumor area to 785 nm. The result showed that abundant ROS were produced at the tumor tissues when treated with CP-NPs under irradiation compared to several control groups, such as vitamin C (Vc) used to scavenge ROS in the tumors (Figure 5F). The authors also measured the *in vivo* ability of CP-NPs to increase temperature using infrared thermograph. Under irradiation, CP-NPs at different doses produced the remarkable temperature elevations ranging from 13 °C to 53 °C (Figure 5G, H). Therefore, CP-NPs can generate ROS in *in vivo* and produce hyperthermia at tumor, leading to increased anticancer efficacy (Figure 5I).

Near infrared light is usually used in PDT, and the effects of PDT and PTT sometimes concurrently happen, thus it is needed to develop novel approaches to quantitatively determine the individual contribution in cancer treatments. For example, Song *et al.* (Song et al., 2017) reported a BSA-MoS_2 nanoparticle conjugated with Cy5.5 that were used for PTT and PDT in cancer treatment. To eliminate PTT effect, the authors studied the cell death after laser irradiation to cells at 4 °C. To avoid PDT effect, the authors used sodium azide (a radical quencher) for cell viability studies. The result showed that the combinatory effect of PTT and PDT contributed to cell death. ICG is the common PDT agent, but it also produces the heat due to absorption of near infrared. It is possible to quantitively measure each contribution of PTT an PDT using the similar methods discussed above. However, it is challenging to determine the individual contribution of PTT or PDT *in vivo*.

2.3 Development of PSs for targeted PDT

Ideal PDT is not only determined by ROS production, but also by the degree of selectivity of PSs to targeted tissues. A PS is the most critical element in PDT. Several generations of PSs have been developed since the first use of hematoporphyrin derivatives to suppress tumor growth in the mouse mammary fat pad in 1975 (Fan et al., 2016). Table 1 summarizes some representative PSs for PDT. Unfortunately, the previous generation of agents showed several

drawbacks including poor specific targeting properties and high toxic side effects (Paszko, Ehrhardt, Senge, Kelleher, & Reynolds, 2011). Therefore, developing new generations of PSs is aimed at designing targeting moieties to PSs to increase the tissue selectivity.

2.3.1 Genetical engineering of PS proteins for targeting and live imaging— Increased selectivity of PSs to tumor tissues are critical for their clinical applications (Josefsen & Boyle, 2008; Leung et al., 2008). In the biological studies, live cell imaging and *in vivo* live animal imaging require genetical engineering of some proteins for targeting subcellular components. For example, some genetically targeted PSs such as KillerRed, ReAsH and mini $^1O_2$ generator (miniSOG) (Bulina et al., 2005; Shu et al., 2011; Tour, Meijer, Zacharias, Adams, & Tsien, 2003; Westberg, Holmegaard, Pimenta, Etzerodt, & Ogilby, 2015), have been engineered to enhance the specificity in living cells. However, few genetically encoded PSs can be excited by light in far-red/NIR wavelengths, therefore deep tissues imaging is limited. He *et al.*(J. He et al., 2016) utilized the genetically targetable fluorogen activating protein (FAP) technology combined with a heavy atom-substituted fluorogenic dye, creating a genetically targeted NIR light-activated PS (TAP) complex for deep tissue penetration. The heavy atom iodine substitutions on the malachite green fluorogen (MG-2I) was needed to enhance the intersystem crossing, so that it increased the yield of $^1O_2$ and facilitated the excitation in the NIR range (Gandin, Lion, & Van de Vorst, 1983; J. He et al., 2016; Yogo, Urano, Ishitsuka, Maniwa, & Nagano, 2005). FAP_{dL5**} in living cell is a highly efficient fluorescence activation tag and it is the binder for MG derivative. MG-2I binds to dL5** in living cells through receptor endocytosis and forms an NIR light-excitable fluorescent complex with the ability to generate $^1O_2$ (Figure 6A). They tested cellular photoablation of FAP-TAPs on various types of HEK293 cells, including mutant cells expressed with a FAP and wildtype cells. The results clearly showed that fluorescently labeled TM-dL5**-expressing HEK cells treated with both MG-2I and laser illumination were dead, whereas the cells expressing FAP treated with free dye and the wild-type HEK cells treated with MG-2I in the illumination field did not show the obvious cytotoxicity (Figure 6B). *In vivo* effectiveness of FAP-TAPs on cardiac cellular ablation in living larval zebrafish expressed with dL5** in the heart (Tg^{pt22}) has been tested as well. The zebrafish embryos were treated with MG-2I or MG-ester in the concentration of 500 nM and then were subjected to laser illumination. At 24 h post-illumination, Tg^{pt22} larvae treated with MG-2I exhibited visibly development defects relative to control groups, such as small eyes and collapsed, large cardiac edema, nonfunctional heart chambers. However, zebrafish developed normally in control groups (Figure 6C), suggesting that MG-2I combined with FAP together is a potent NIR light-excitable PS to cause a regenerative response *in vivo*. The FAP_{dL5**} or TAPs (MG-2I) alone showed no photosensitizing ability. This study indicates that PSs can be genetically engineered and activated by light in the NIR range to induce cytotoxicity. This novel approach offers the opportunity to specifically damage the subcellular organelles in live tissues to understand biological properties in the response to ROS.

2.3.2 Surface-functionalized aggregation-induced emission (AIE) dots used in PDT—In traditional PSs, limited ROS production can be caused by fluorescence quenching of PSs because their hydrophobic characteristics and planar structures facilitate

the aggregation in fluids. PSs generated by aggregation-induced emission (AIE) could overcome this drawback in fluorescence quenching. Fluorogens with AIE characteristics (AIEgens) exhibit nonradiative decay and show bright fluorescence in the aggregate state due to the restriction of intramolecular motions (RIM) (Hu, Xu, & Liu, 2018).

Tumor tissues are usually comprised of leaky vasculature, so nanoparticles spontaneously accumulate in tumor sites rather than in healthy tissues. Passive targeting to tumors was proposed based on enhanced permeability and retention (EPR) effect when nanoparticles have a long circulation time (Bertrand, Wu, Xu, Kamaly, & Farokhzad, 2014; Chu, Dong, Shi, Zhang, & Wang, 2018; A. Z. Wang, Langer, & Farokhzad, 2012). While the passive targeting of nanoparticles is used in cancer treatment, the tumor deposition of nanoparticles is limited. In contrast, active targeting of PSs to diseased sites was proposed by biofunctionalization of nanoparticles. The idea was that various targeting ligands (e.g. an antibody) were decorated on the surface of nanoparticles to recognize specific receptors highly expressed on tumor cells, thus enhancing the uptake of nanoparticles by tumor cells (Bazak, Houri, El Achy, Kamel, & Refaat, 2015; Byrne, Betancourt, & Brannon-Peppas, 2008; F. Chen et al., 2013; Hong et al., 2012; Kamkaew, Chen, Zhan, Majewski, & Cai, 2016).

To significantly deliver PSs into tumor tissues, ligands that target special biomarkers highly expressed on tumor cells can be conjugated to PS molecules. Li *et al.* took advantage of a red emissive AIE PS 2-(2,6-bis((E)-4-(phenyl(4'-(1,2,2-triphenylvinyl)-[1,1'-biphenyl]-4-yl)amino)styryl)-4*H*-pyran-4-ylidene)malononitrile (TTD) to create an integrin $\alpha_V\beta_3$ targeted AIE dot (T-TTD dot) for PDT in a cholangiocarcinoma mouse model (M. Li et al., 2017). TTD showed AIE with bright fluorescence when it was aggregated, but it was non-emissive when it was in an isolated molecular state. Compared to traditional PSs and PSs-loaded nanoparticles, T-TTD dots did not suffer from rapid fluorescence quenching and dramatic reduction of ROS production. Cyclic-Arg-Gly-Asp (cRGD) peptide is a targeting ligand for $\alpha_V\beta_3$ integrin protein overexpressed in certain cancers. Figure 7A represents the hypothesis for development of the targeted PDT to treat cholangiocarcinoma tumor. After ~40 nm-sized T-TTD dots were intravenously injected to a tumor-bearing mouse, they specifically targeted the tumor tissue by EPR effect. The nanoparticle uptake by tumor cells was dependent on ligand-receptor-mediated endocytosis because cRGD peptide on dots can bind to integrin $\alpha_V\beta_3$ on tumors. Subsequently, the tumor area was exposed to light and the red fluorescence emitted by T-TTD dots displayed the tumor margin and PDT directly ablated the tumor. To evaluate the targeting ability of T-TTD dots to cholangiocarcinoma tumor, confocal laser scanning microscopy (CLSM) showed (as shown in Figure 7B) a strong red fluorescence observed in QBC 939 cells, however the fluorescent signal in the normal L-O2 and HK-2 cells was negligible, suggesting the specific internalization of T-TTD dots by QBC939 cells. Next, blocking experiments were conducted *in vivo* to confirm the ligand-receptor binding specificity. After cilengitide (integrin $\alpha_V\beta_3$ inhibitor) was administered followed by the injection of T-TTD dots, the result showed that the combination therapy dramatically decreased tumor growth, indicating that T-TTD dots modified with cRGD targeting ligands can facilitate tumor accumulation (Figure 7C). The significant antitumor effect has been achieved when the tumor was exposed to light (Figure 7D).

2.4 PDT combined with cancer immunotherapies

Tumor microenvironment is a unique system including vasculature to transport nutrients for tumor growth and residence of immune cells to suppress the host immune defense to eliminate tumor cells. Manipulation of tumor microenvironments is a novel strategy to increase the infiltration of immune cells to a tumor site. Hijacking immune cells would increase the drug delivery of PSs, thus enhancing PDT. In the section, we will introduce a new concept that PDT can be utilized to generate acute inflammation in tumor tissues to mediate neutrophil transmigration from circulation to the tumors (Chu et al., 2018; Dong et al., 2017, 2018). Neutrophils are the most abundant white blood cells in humans, occupying 40–75% (Nauseef & Borregaard, 2014). They are the first line of defense against invasion of bacteria and viruses, playing a central role to maintain the homeostasis. Neutrophils are a major component of acute inflammation. Inflammation is a host protection process against tissue injury and infections. In acute inflammation, neutrophils are activated in circulation and migrate across blood vessels to move to infectious or injured sites (J. Gao, Chu, & Wang, 2016; J. Gao, Wang, & Wang, 2017). Although tumor microenvironments contain immune cells, it is difficult to target these immune cells because of blood vessel barriers and random movements of immune cells. In order to increase delivery of nanotherapeutics including PSs into tumors, a new concept has been proposed that acute inflammation induced by PDT or antibodies mediate the tumor filtration of neutrophils. We will discuss two examples to illustrate the importance of combined therapies of PDT and immune priming of tumor microenvironments.

2.4.1 Photosensitization priming of tumor microenvironments mediates delivery of nanoparticles via neutrophils—PDT is involved with the generation of ROS. ROS is a mediator to promote inflammation (Chu, Dong, Zhao, Gu, & Wang, 2017). The inflammation is the immune response of the host to infections and tissue injury. The characteristic of acute inflammation is the activation of neutrophils in circulation, and neutrophils bind to activated blood endothelium and transmigrate into the inflamed tissues via crossing blood vessel barrier (Chu et al., 2018). Although the innovations in synthesis and engineering of nanoparticles allow to increase targeted delivery of drugs, blood vessel barrier is still an issue to translate nanotechnology in cancer therapies (Z. Wang & Malik, 2013; Z. Wang et al., 2011; Z. Wang et al., 2009). PDT can spontaneously promote tissue inflammation because of ROS production. There are many opportunities to combine PDT with associated immune responses to develop synergistic methods for cancer therapies.

Chu *et al.* reported a novel strategy where photosensitization can activate neutrophil recruitment to facilitate the delivery of nanoparticles across tumor blood vessel barrier (Chu et al., 2017). In this study, the PS pyropheophorbide-a (Ppa) was administered into a tumor-bearing mouse *via* tail vain, followed by exposure of tumor region with the light to produce ROS that induces acute inflammation in tumor tissues. Subsequently, neutrophils containing nanoparticles rapidly transmigrated into deep tumor tissues in response of acute inflammation (Figure 8A). During acute inflammation, CD11b highly expressed on activated neutrophils in circulation. After injection of anti-CD11b-coated nanoparticles (NPs-anti-CD11b), they were rapidly internalized by neutrophils through the receptor-mediatied endocytosis. Neutrophils containing NPs-anti-CD11b migrated into the tumor due to their

tissue infiltration feature. Figure 8B clearly displayed that NPs-anti-CD11b were taken up by neutrophils, residing outside of the blood vessel. Comparing to a series of control experiments, photosensitization and anti-CD11b ligands were needed for transport of nanoparticles into tumors (Figure 8C, D). Figure 8E shows that nanoparticle movement was inhibited when neutrophils were depleted by injection of anti-LY-6G antibody. To address whether neutrophils can be a carrier to deliver therapeutics for cancer therapies, the authors conjugated anti-CD11b to gold nanorods (GNRs) (GNRs-anti-CD11b) because GNRs can generate the heat to kill tumor cells. When GNRs-anti-CD11b were given to a tumor-bearing mouse, the tumor tissue temperatures dramatically increased after the exposure of laser (Figure 8F, G). The comparison with several controls (different coating of nanoparticles and photosensitization) shows that neutrophil tumor infiltration is required to enhance the tumor tissue temperatures. To demonstrate the usefulness of this new cancer therapy platform, the authors studied the tumor growth and mouse survival after treatment of GNRs-anti-CD11b. The results (Figure 8H and I) demonstrated that targeting of activated neutrophils in situ using bio-conjugated nanoparticles is the useful method to deliver therapeutics into tumor tissues. This study also shows that combination of PDT with neutrophil-mediated delivery of nanotherapeutics may improve the current cancer therapies.

2.4.2 PDT combined with neutrophil immunotherapy—Immunotherapy is a powerful tool to initiate the innate and adaptive responses to recognize tumor cells (Mellman, Coukos, & Dranoff, 2011). In the past decade, monoclonal antibodies are major biologic therapies for cancer treatment. The idea is that specific tumor antigens are targeted by antibodies, for example, anti-HER-2 mAb trastuzumab applied to treat breast cancer shows the benefit (Hudis, 2007).

In a B16 melanoma-bearing mouse, monoclonal antibody TA99 specific to gp75 antigen expressed on tumor cells can promote neutrophil tumor infiltration based on antibody-dependent cell-mediated cytotoxicity (ADCC) for cancer immunotherapy (Albanesi et al., 2013). It is found that neutrophils play a crucial role in this immunotherapy. Recent studies show that albumin nanoparticles can specifically bind to activated neutrophils and deliver anti-inflammation agents to infectious tissues. Chu *et al.* hypothesized whether they can utilize neutrophils to mediate the delivery of PSs for improved PDT (Chu et al., 2016). In Figure 9A, it is noted that the content of neutrophils in tumor cells was significantly boosted 48 h after the administration of TA99. The authors assumed that if nanoparticles can be internalized by neutrophils *in vivo*, the neutrophils would carry a therapeutic into tumors for cancer therapy. By taking the advantage of fluorescence confocal microscopy, the authors observed that albumin nanoparticles can be taken up by activated neutrophils in the presence of TA99, while in the absence of TA99, there were negligible neutrophils that internalized albumin nanoparticles (Figure 9B). The further study showed that the presence of TA99 dramatically enhanced the concentration of nanoparticles in tumors compared to those in the absence of TA99 and when neutrophils were abolished (Figure 9C), indicating that nanoparticle delivery was strongly dependent on neutrophil tumor infiltration. To examine the effectiveness of PDT in cancer treatment, the authors loaded PS Ppa in albumin nanoparticles and administered to tumor-bearing mice along with TA99, tumor growth was

dramatically suppressed and mouse survival was increased compared to the treatments with the nanoparticles alone or TA99 alone (Figure 9D, E).

3. PDT in infectious diseases

An emerging research area in PDT is to fight infectious diseases. The current issue in bacterial infections is that bacteria rapidly develop multi-drug resistance for new antibiotics (Wainwright et al., 2017), therefore it is urgent to seek novel antimicrobial approaches totally different from traditional development of antibiotics. There are two major molecular mechanisms regulating antibiotic resistance: 1) Intrinsic or natural resistance of antibiotics where microorganisms do not have the target sites for the drugs, or they have low bacterial permeability to antibiotics. 2) Acquired resistance where microorganisms develop defense mechanisms to prevent the entrance of antibiotics. While antimicrobial resistance is a natural existence of biological properties, it is often increased as a result of the adaption forced upon microbes by continuous or repeated exposure to antibiotics used to prevent or treat infections in humans or other species. It is recognized that excessive antibiotic use is the most important factor contributing to increased antimicrobial resistance (Y. Wang et al., 2017). Targeted delivery of antibiotics to infectious tissues may be a novel strategy to diminish antibiotic resistance. A recent study showed that nanoparticles coated with ICAM-1 antibody can specifically target infectious microenvironments to deliver antibiotic (ciprofloxacin) to treat sepsis and acute lung infections induced by *P. aeruginosa* (C. Y. Zhang, Gao, & Wang, 2018).

While this result demonstrates a new direction to solve the current crisis on antibiotic resistance, many fundamental issues still remain. PDT used in killing bacteria is a new concept to develop novel approaches to fight infections because PDT has the natural features to prevent bacteria from developing drug resistance (Spellberg, Bartlett, & Gilbert, 2013). To develop effective antimicrobial PDT therapy, it is required that PS should precisely target to microbial cells (Malik, Ladan, & Nitzan, 1992). In general, microbial cells are more negatively charged relative to mammalian cells, therefore positively charged PS can selectively and firmly bind to microbial cell membrane, thus avoiding the binding of PS to host mammalian cells (Hamblin, 2016). Since biological systems are so complicated, the trafficking and bio-distribution of PS may be difficult to predict. Therefore, designing nanoparticle-based carriers may control the trafficking of PS and improve antimicrobial therapy compared to free PS.

In this section, we describe several examples to illustrate the design of new nanomaterials to target infectious tissues for improved treatments of infectious diseases. Finally, we discuss the potential issue in microbial resistance to PDT-induced oxidative stress.

3.1 Inhibiting bacterial multidrug-resistance using AIE luminogen

Multidrug-resistant (MDR) bacteria are severe microorganisms that may cause the deaths due to ineffectiveness of antibiotics. It is urgent to develop a new method to kill MDT bacteria that is independent on antibiotics. PDT is a physical approach to deactivate bacterial activities via the generation of ROS in bacteria.

The recent study demonstrated that a PS made of a bifunctional aggregation-induced emission luminogen (AIEgen) can generate ROS to kill Gram-positive and Gram-negative bacteria (Y. Li et al., 2018). We have discussed that AIEgen displays weak fluorescence as isolated molecules in liquid, however the fluorescence was enhanced in the aggregated state of AIEgen. This feature allows the high production of ROS and bioimaging. Specifically, AIEgen, triphenylthylene-naphthalimide triazole (TriPE-NT) is composed of triphenylethylene (TriPE) connected to naphthalimide triazole (NT) to form positively charged TriPE-NT. The authors assessed the AIEgen characteristics by measuring a PL intensity after water was added to tetrahydrofuran (THF) at the different ratios. It was observed that the fluorescence of TriPE-NT was strongly dependent on the water addition, and the fluorescence reached to maximum when the water at 90% (Figure 10A). The result suggested that the bright emission was due to the aggregation of TriPE-NT, and accordingly the size of TriPE-NT was 30 nm in diameter. In addition, TriPE-NT can generate ROS measured by a ROS indicator, dichlorofluorescein (DCFH) upon the light irradiation (Figure 10B). Furthermore, TriPE-NT was evaluated in wild types and MDR bacteria of *Escherichia coli* (*E. coli*) and *Staphylococcus epidermidis* (*S. epidermidis*), showing the enhanced bacterial killing. The results in Figure 10C and D show that TriPE-NT can kill both Gram-positive and Gram-negative wild and MDR bacteria because of antimicrobial agents NT in TriPE-NT without the light irradiation. However, the exposure to light enhanced the antibacterial ability of TriPE-NT, implying that PDT generated ROS to improve bacterial killing. Furthermore, the authors performed *in vivo* antibacterial effects of TriPE-NT in rat bacteria-infected wound model. They measured the sizes of wounds 3 days and 7 days after the treatment with TriPE-NT and light irradiation. The results showed the significant wound reduction after PDT, indicating the potent antimicrobial effect of TriPE-NT (Figure 10E and F).

3.2 PTT/PDT synergetic function in advanced bacteria-infected wound therapy

Gao *et al.* reported a novel antimicrobial nanotherapeutic, MoS_2-BNN6 comprised of N, N'-di-sec-butyl-N, N'-dinitroso-1,4-phenylenediamine (BNN6) loaded in α-cyclodextrin (α-CD) and molybdenum sulfide (MoS_2), can be used to build the combined therapies of PTT and NIR laser triggered releasing of nitric oxide (NO) for antibacterial therapy (Figure 11A) (Q. Gao et al., 2018). BNN6 is a heat-sensitive NO donor and MoS_2 serves as the photothermal agent and nanocarrier. Under NIR irradiation, hyperthermia generated from MoS_2-BNN6 controlled the release of NO specifically in targeted bacteria. NO can kill a broad range of bacteria through several mechanism, such as NO as a signaling molecule to initiate immune response against infection and reactive nitrogen species (RNS) produced by NO directly bind DNA. Furthermore, NO can help the reconstruction of collagen and myofibroblast in wound healing. The combination of PTT and NO antibacterial function could be a novel strategy to kill antibiotic-resistant bacteria. Inspired by this idea, the authors evaluated the bactericidal effect of MoS_2-BNN6 in ampicillin resistant *Escherichia coli* (Amp^r *E. coli*) and heat-resistant *Escherichia faecalis* (*E. faecalis*) bacteria. Figure 11B shows that MoS_2-BNN6 obviously decreased the colony numbers of two type antibiotics-resistant bacteria under light irradiation. The wound healing experiments (Figure 11C and D) showed that MoS_2-BNN6 was more potent than several control groups in bacterial

infections, and this therapy platform was safe, demonstrating a new strategy to treat bacterial infections.

3.3 Antimicrobial resistance to PDT-induced oxidative stress

PDT approaches theoretically do not develop antibiotic resistance because antibiotics are not used in PDT. However, the recent studies showed that there was the potential for bacteria to develop the resistance to PDT-induced oxidative stress. Oxidative stress occurs when the level of ROS accumulation exceeds the bacterial scavenger ability. Bacteria have the ability to respond to oxidative stress, such as activate protective systems that can fix oxidative damage, limit the concentration of Fe^{2+} and protect susceptible enzymes from inactivation (Taylor, Stapleton, & Paul Luzio, 2002). PDT attacks bacteria through ROS, the PS is not required to enter into bacteria, which further prevent the chance develop resistance to PDT (Almeida, Faustino, & Tome, 2015). Additionally, we know that the efflux system is a major component for antimicrobial resistance because bacteria can remove exogenous toxic substrates like antibiotics out of cells (Webber & Piddock, 2003). Efflux systems are transport proteins, therefore it is worth to emphasize that proteins are major susceptible targets of PDT (Alves et al., 2014). Giuliani et al. examined whether bacteria can develop the resistance to a specific agent in PDT by continually exposing bacteria to the agent (Giuliani et al., 2010). They found that after 20 repetitive exposure to tetracationic PS Zn (II) phthalocyanine derivative under 30 J/cm^2 of 600–700 nm light, Gram-positive bacteria *Staphylococcus aureus*, and Gram-negative bacteria *Pseudomonas aeruginosa* were both unable to develop resistance to the agent. When treated without light, the minimum inhibitory PS concentration for *S. aureus* increased. This indicates that *S.aureus* possibly developed some ability to protect itself from the damage induced by PS in the low light.

4. CONCLUSIONS AND PERSPECTIVES

PDT has demonstrated the usefulness in cancer therapies because of several features, such as minimal invasiveness, harmless, feasibility, high selectivity and efficiency (D. E. J. G. J. Dolmans, D. Fukumura, & R. K. Jain, 2003; Z. Huang, 2005). To improve the delivery efficiency and tissue specificity of PSs, many nanoparticle-based formulations have been proposed and developed. In this Review, we are focused on the recent innovations in nanoparticle engineering and rational design of new PSs. For example, design of new PSs is to increase the light absorption efficiency and ROS generation. Conjugated polymer-based and D-A system-based new PSs have been developed. In the future, organic chemistry and materials sciences will play a central role in improving the design of PSs. In addition, tissue oxygen contents in tumors are critical to enhance the ROS generation. We have described two examples where inorganic materials (lanthanides and Fe3+/Cu2+) were used to generate ROS that is not dependent on tissue oxygen. It is interesting to design conjugated polymer-based PS nanoparticles that can respond to tumor microenvironments. We believe that there are more rooms to develop new nanomaterials that are responsive to tumor microenvironments, and photosensitization process is controlled by material properties and tissue physiology.

Genetically engineering PS-protein complexes is a new direction for live cell imaging and intravital microscopy. Coupling of a PS to a protein in a cell is to localize light to activate cellular functions in the subcellular component. Local ROS generation can be exploited to investigate signaling pathways to contribute inflammation responses. Because protein expression is specific in the locations of a cell, PDT may promote the targeted damage of organelles in a cell. We believe that this tool will be benefit to biologists to address the basic cellular biology.

Most exciting is that PDT can be combined to cancer immunotherapies. Here, we only described two examples where PDT is a tool to initiate acute inflammation in tumor tissues. Neutrophil tumor infiltration has been utilized to deliver albumin nanoparticles (Chu et al., 2016) and gold nanoparticles (Chu et al., 2017). The data are promising and strongly support the new concept of synergistic therapies of PDT and immunotherapies. Tumor microenvironments are unique tissues including vasculature and immune cells. How we combine PDT and tumor immunology for cancer therapies is a very interesting and exciting question. We believe that there are many opportunities to explore the role of PDT in cancer immunotherapies.

Bacteria rapidly develop antibiotic resistance, thus it is urgent to develop new therapeutics that do not promote antimicrobial resistance. For example, PDT is the physical method to generate ROS to destroy bacteria, so-called antimicrobial photodynamic inactivation (aPDI). The novel feature of aPDI may prevent antibiotic resistance because PSs do not show the acquired drug resistance as antibiotics do. In addition, production of ROS by PDT can act multiple targets in bacteria, such as lipids, proteins, and DNA, thus avoiding the drug resistance development (Spellberg et al., 2013). We have discussed a recent study to show that AIE luminogens can increase ROS production to dramatically kill a wide range of bacteria. In addition, the integration of PTT/PDT provides a promising method to effectively kill antibiotic resistant bacteria in the wound mouse model. We expect that new nanomaterials will improve the current therapies in infectious diseases.

Pathogenesis of cancers and infectious diseases has the similarity because it is strongly dependent on the host immune responses. Vascular inflammation plays a central role in the disease developments. Recent studies show that targeting inflamed vasculature is a novel strategy to specifically deliver therapeutics to diseased lesions. In inflammatory sites, blood vessel endothelium highly expresses intercellular adhesion molecules (such as ICAM-1) that recruit neutrophils (a type of white blood cells) in response to infections. In the studies, Gao *et al* proposed to generate nanovesicles directly made from neutrophil membrane using nitrogen cavitation, and showed that the nanovesicles can specifically deliver antibiotics and anti-inflammatory agents in inflammation sites in lung infections (J. Gao et al., 2016; J. Gao et al., 2017) and stroke (Dong et al., 2019). In addition, Zhang *et al* designed pH-responsive polymer micelles coated with anti-ICAM-1 to treat sepsis and acute lung injury induced by bacteria (C. Y. Zhang et al., 2018). These studies show that neutrophil membrane derived nanovesicles and bio-conjugated nanoparticles may be the good carriers to deliver photosensitizers to cancer tissues and infectious sites, thus improving PDT therapies in cancer and infectious diseases.

In summary, the current developments in design of new nanomaterials, genetic engineering of a PS and PDT-priming of tumor microenvironments show the promising therapies to cancers. In addition, the new application of PDT in infectious diseases may avoid the antibiotic resistance that is a threat to the globe epidemic. We expect that the advances in nanotechnology, materials engineering and immunology may offer the translation of PDT to improve current therapies in cancers and infectious diseases.

Acknowledgements

This work was supported by National Institute of Health RO1GM116823 to Z.W.

References

Abbas M, Zou Q, Li S, & Yan X (2017). Self-Assembled Peptide- and Protein-Based Nanomaterials for Antitumor Photodynamic and Photothermal Therapy. Adv Mater, 29(12). doi:10.1002/adma.201605021

Abrahamse H, & Hamblin MR (2016). New photosensitizers for photodynamic therapy. Biochem J, 473(4), 347–364. doi:10.1042/bj20150942 [PubMed: 26862179]

Agostinis P, Berg K, Cengel KA, Foster TH, Girotti AW, Gollnick SO, … Hamblin MR (2011). PHOTODYNAMIC THERAPY OF CANCER: AN UPDATE. 61(4), 250–281. doi:10.3322/caac.20114

Agostinis P, Berg K, Cengel KA, Foster TH, Girotti AW, Gollnick SO, … Golab J (2011). PHOTODYNAMIC THERAPY OF CANCER: AN UPDATE. CA Cancer J Clin, 61(4), 250–281. doi:10.3322/caac.20114 [PubMed: 21617154]

Ai F, Ju Q, Zhang X, Chen X, Wang F, & Zhu G (2015). A core-shell-shell nanoplatform upconverting near-infrared light at 808 nm for luminescence imaging and photodynamic therapy of cancer. Sci Rep, 5. doi:10.1038/srep10785

Albanesi M, Mancardi DA, Jonsson F, Iannascoli B, Fiette L, Di Santo JP, … Bruhns P (2013). Neutrophils mediate antibody-induced antitumor effects in mice. Blood, 122(18), 3160–3164. doi:10.1182/blood-2013-04-497446 [PubMed: 23980063]

Almeida A, Faustino MA, & Tome JP (2015). Photodynamic inactivation of bacteria: finding the effective targets. Future Med Chem, 7(10), 1221–1224. doi:10.4155/fmc.15.59 [PubMed: 26144260]

Alves E, Faustino MA, Neves MG, Cunha A, Tome J, & Almeida A (2014). An insight on bacterial cellular targets of photodynamic inactivation. Future Med Chem, 6(2), 141–164. doi:10.4155/fmc.13.211 [PubMed: 24467241]

Ancona A, Dumontel B, Garino N, Demarco B, Chatzitheodoridou D, Fazzini W, … Cauda V (2018). Lipid-Coated Zinc Oxide Nanoparticles as Innovative ROS-Generators for Photodynamic Therapy in Cancer Cells. Nanomaterials (Basel), 8(3). doi:10.3390/nano8030143

Bazak R, Houri M, El Achy S, Kamel S, & Refaat T (2015). Cancer active targeting by nanoparticles: a comprehensive review of literature. J Cancer Res Clin Oncol, 141(5), 769–784. doi:10.1007/s00432-014-1767-3 [PubMed: 25005786]

Bellnier DA, Greco WR, Loewen GM, Nava H, Oseroff AR, & Dougherty TJ (2006). Clinical pharmacokinetics of the PDT photosensitizers porfimer sodium (Photofrin), 2-[1-hexyloxyethyl]-2-devinyl pyropheophorbide-a (Photochlor) and 5-ALA-induced protoporphyrin IX. Lasers Surg Med, 38(5), 439–444. doi:10.1002/lsm.20340 [PubMed: 16634075]

Bertrand N, Wu J, Xu X, Kamaly N, & Farokhzad OC (2014). Cancer nanotechnology: the impact of passive and active targeting in the era of modern cancer biology. Adv Drug Deliv Rev, 66, 2–25. doi:10.1016/j.addr.2013.11.009 [PubMed: 24270007]

Bhana S, O'Connor R, Johnson J, Ziebarth JD, Henderson L, & Huang X (2016). Photosensitizer-loaded gold nanorods for near infrared photodynamic and photothermal cancer therapy. J Colloid Interface Sci, 469, 8–16. doi:10.1016/j.jcis.2016.02.012 [PubMed: 26866884]

Bulina ME, Chudakov DM, Britanova OV, Yanushevich YG, Staroverov DB, Chepurnykh TV, … Lukyanov KA (2005). A genetically encoded photosensitizer. Nat Biotechnol, 24, 95. doi:10.1038/nbt117510.1038/nbt1175https://www.nature.com/articles/nbt1175#supplementary-informationhttps://www.nature.com/articles/nbt1175#supplementary-information [PubMed: 16369538]

Byrne JD, Betancourt T, & Brannon-Peppas L (2008). Active targeting schemes for nanoparticle systems in cancer therapeutics. Adv Drug Deliv Rev, 60(15), 1615–1626. doi:10.1016/j.addr.2008.08.005 [PubMed: 18840489]

Castano AP, Mroz P, & Hamblin MR (2006). Photodynamic therapy and anti-tumour immunity. Nat Rev Cancer, 6(7), 535–545. doi:10.1038/nrc1894 [PubMed: 16794636]

Chandel NS (2014). Mitochondria and cancer. Cancer & Metabolism, 2, 8–8. doi:10.1186/2049-3002-2-8 [PubMed: 24917929]

Chen F, Hong H, Zhang Y, Valdovinos HF, Shi S, Kwon GS, … Cai W (2013). In vivo tumor targeting and image-guided drug delivery with antibody-conjugated, radiolabeled mesoporous silica nanoparticles. ACS Nano, 7(10), 9027–9039. doi:10.1021/nn403617j [PubMed: 24083623]

Chen H, Wang GD, Chuang YJ, Zhen Z, Chen X, Biddinger P, … Xie J (2015). Nanoscintillator-mediated X-ray inducible photodynamic therapy for in vivo cancer treatment. Nano Lett, 15(4), 2249–2256. doi:10.1021/nl504044p [PubMed: 25756781]

Chen Q, Xu L, Liang C, Wang C, Peng R, & Liu Z (2016). Photothermal therapy with immune-adjuvant nanoparticles together with checkpoint blockade for effective cancer immunotherapy. Nat Commun, 7, 13193. doi:10.1038/ncomms13193 [PubMed: 27767031]

Chu D, Dong X, Shi X, Zhang C, & Wang Z (2018). Neutrophil-Based Drug Delivery Systems. Adv Mater, 30(22), e1706245. doi:10.1002/adma.201706245 [PubMed: 29577477]

Chu D, Dong X, Zhao Q, Gu J, & Wang Z (2017). Photosensitization Priming of Tumor Microenvironments Improves Delivery of Nanotherapeutics via Neutrophil Infiltration. Adv Mater, 29(27). doi:10.1002/adma.201701021

Chu D, Zhao Q, Yu J, Zhang F, Zhang H, & Wang Z (2016). Nanoparticle Targeting of Neutrophils for Improved Cancer Immunotherapy. Adv Healthc Mater, 5(9), 1088–1093. doi:10.1002/adhm.201500998 [PubMed: 26989887]

Dang J, He H, Chen D, & Yin L (2017). Manipulating tumor hypoxia toward enhanced photodynamic therapy (PDT). Biomater Sci, 5(8), 1500–1511. doi:10.1039/c7bm00392g [PubMed: 28681887]

Derosa M, & J Crutchley R (2002). Photosensitized Singlet Oxygen and Its Applications (Vol. 233–234).

DeRosa MC, & Crutchley RJ (2002). Photosensitized singlet oxygen and its applications. Coordination Chemistry Reviews, 233–234, 351–371. doi:10.1016/S0010-8545(02)00034-6

Dolmans DE, Fukumura D, & Jain RK (2003). Photodynamic therapy for cancer. Nat Rev Cancer, 3(5), 380–387. doi:10.1038/nrc1071 [PubMed: 12724736]

Dolmans DEJGJ, Fukumura D, & Jain RK (2003). Photodynamic therapy for cancer. Nature Reviews Cancer, 3, 380. doi:10.1038/nrc1071 [PubMed: 12724736]

Dong X, Chu D, & Wang Z (2017). Leukocyte-mediated Delivery of Nanotherapeutics in Inflammatory and Tumor Sites. Theranostics, 7(3), 751–763. doi:10.7150/thno.18069 [PubMed: 28255364]

Dong X, Chu D, & Wang Z (2018). Neutrophil-mediated delivery of nanotherapeutics across blood vessel barrier. Ther Deliv, 9(1), 29–35. doi:10.4155/tde-2017-0081 [PubMed: 29216803]

Dong X, Gao J, Zhang CY, Hayworth C, Frank M, & Wang Z (2019). Neutrophil Membrane-Derived Nanovesicles Alleviate Inflammation To Protect Mouse Brain Injury from Ischemic Stroke. ACS Nano. doi:10.1021/acsnano.8b06572

Dougherty TJ, Grindey GB, Fiel R, Weishaupt KR, & Boyle DG (1975). Photoradiation therapy. II. Cure of animal tumors with hematoporphyrin and light. J Natl Cancer Inst, 55(1), 115–121. [PubMed: 1159805]

Du L, Qin H, Ma T, Zhang T, & Xing D (2017). In Vivo Imaging-Guided Photothermal/Photoacoustic Synergistic Therapy with Bioorthogonal Metabolic Glycoengineering-Activated Tumor Targeting Nanoparticles. ACS Nano, 11(9), 8930–8943. doi:10.1021/acsnano.7b03226 [PubMed: 28892360]

Durantini AM, Greene LE, Lincoln R, Martinez SR, & Cosa G (2016). Reactive Oxygen Species Mediated Activation of a Dormant Singlet Oxygen Photosensitizer: From Autocatalytic Singlet Oxygen Amplification to Chemicontrolled Photodynamic Therapy. J Am Chem Soc, 138(4), 1215–1225. doi:10.1021/jacs.5b10288 [PubMed: 26789198]

Ethirajan M, Chen Y, Joshi P, & Pandey RK (2011). The role of porphyrin chemistry in tumor imaging and photodynamic therapy. Chem Soc Rev, 40(1), 340–362. doi:10.1039/b915149b [PubMed: 20694259]

Fan W, Huang P, & Chen X (2016). Overcoming the Achilles' heel of photodynamic therapy. Chem Soc Rev, 45(23), 6488–6519. doi:10.1039/c6cs00616g [PubMed: 27722560]

Feder ME, & Hofmann GE (1999). Heat-shock proteins, molecular chaperones, and the stress response: evolutionary and ecological physiology. Annu Rev Physiol, 61, 243–282. doi:10.1146/annurev.physiol.61.1.243 [PubMed: 10099689]

Gandin E, Lion Y, & Van de Vorst A (1983). QUANTUM YIELD OF SINGLET OXYGEN PRODUCTION BY XANTHENE DERIVATIVES. Photochem Photobiol, 37(3), 271–278. doi:doi:10.1111/j.1751-1097.1983.tb04472.x

Gao J, Chu D, & Wang Z (2016). Cell membrane-formed nanovesicles for disease-targeted delivery. J Control Release, 224, 208–216. doi:10.1016/j.jconrel.2016.01.024 [PubMed: 26778696]

Gao J, Wang S, & Wang Z (2017). High yield, scalable and remotely drug-loaded neutrophil-derived extracellular vesicles (EVs) for anti-inflammation therapy. Biomaterials, 135, 62–73. doi:10.1016/j.biomaterials.2017.05.003 [PubMed: 28494264]

Gao Q, Zhang X, Yin W, Ma D, Xie C, Zheng L, … Zhao Y (2018). Functionalized MoS2 Nanovehicle with Near-Infrared Laser-Mediated Nitric Oxide Release and Photothermal Activities for Advanced Bacteria-Infected Wound Therapy. Small, 14(45), e1802290. doi:10.1002/smll.201802290 [PubMed: 30307703]

Giuliani F, Martinelli M, Cocchi A, Arbia D, Fantetti L, & Roncucci G (2010). In Vitro Resistance Selection Studies of RLP068/Cl, a New Zn(II) Phthalocyanine Suitable for Antimicrobial Photodynamic Therapy. Antimicrobial Agents and Chemotherapy, 54(2), 637–642. doi:10.1128/aac.00603-09 [PubMed: 20008782]

Guo M, Mao H, Li Y, Zhu A, He H, Yang H, … Chen H (2014). Dual imaging-guided photothermal/photodynamic therapy using micelles. Biomaterials, 35(16), 4656–4666. doi:10.1016/j.biomaterials.2014.02.018 [PubMed: 24613048]

Hamblin MR (2016). Antimicrobial photodynamic inactivation: a bright new technique to kill resistant microbes. Curr Opin Microbiol, 33, 67–73. doi:10.1016/j.mib.2016.06.008 [PubMed: 27421070]

Han J, Park W, Park SJ, & Na K (2016). Photosensitizer-Conjugated Hyaluronic Acid-Shielded Polydopamine Nanoparticles for Targeted Photomediated Tumor Therapy. ACS Appl Mater Interfaces, 8(12), 7739–7747. doi:10.1021/acsami.6b01664 [PubMed: 26965036]

He H, Lo P-C, Yeung S-L, Fong W-P, & Ng DKP (2011). Synthesis and in Vitro Photodynamic Activities of Pegylated Distyryl Boron Dipyrromethene Derivatives. Journal of Medicinal Chemistry, 54(8), 3097–3102. doi:10.1021/jm101637g [PubMed: 21417218]

He J, Wang Y, Missinato MA, Onuoha E, Perkins LA, Watkins SC, … Bruchez MP (2016). A genetically targetable near-infrared photosensitizer. Nat Methods, 13(3), 263–268. doi:10.1038/nmeth.3735 [PubMed: 26808669]

He SJ, Cao J, Li YS, Yang JC, Zhou M, Qu CY, … Xu LM (2016). CdSe/ZnS quantum dots induce photodynamic effects and cytotoxicity in pancreatic cancer cells. World J Gastroenterol, 22(21), 5012–5022. doi:10.3748/wjg.v22.i21.5012 [PubMed: 27275093]

Hong H, Yang K, Zhang Y, Engle JW, Feng L, Yang Y, … Cai W (2012). In vivo targeting and imaging of tumor vasculature with radiolabeled, antibody-conjugated nanographene. ACS Nano, 6(3), 2361–2370. doi:10.1021/nn204625e [PubMed: 22339280]

Hu F, Xu S, & Liu B (2018). Photosensitizers with Aggregation-Induced Emission: Materials and Biomedical Applications. Adv Mater, 30(45), e1801350. doi:10.1002/adma.201801350 [PubMed: 30066341]

Huang L, Li Z, Zhao Y, Yang J, Yang Y, Pendharkar AI, … Han G (2017). Enhancing Photodynamic Therapy through Resonance Energy Transfer Constructed Near-Infrared Photosensitized Nanoparticles. Adv Mater, 29(28). doi:10.1002/adma.201604789

Huang YY, Sharma SK, Yin R, Agrawal T, Chiang LY, & Hamblin MR (2014). Functionalized fullerenes in photodynamic therapy. J Biomed Nanotechnol, 10(9), 1918–1936. doi:10.1166/jbn.2014.1963 [PubMed: 25544837]

Huang Z (2005). A Review of Progress in Clinical Photodynamic Therapy. Technol Cancer Res Treat, 4(3), 283–293. [PubMed: 15896084]

Huang Z, Chen Q, Dole KC, Barqawi AB, Chen YK, Blanc D, … Hetzel FW (2007). The effect of Tookad-mediated photodynamic ablation of the prostate gland on adjacent tissues - in vivo study in a canine model. Photochem Photobiol Sci, 6(12), 1318–1324. doi:10.1039/b705984a [PubMed: 18046488]

Hudis CA (2007). Trastuzumab--mechanism of action and use in clinical practice. N Engl J Med, 357(1), 39–51. doi:10.1056/NEJMra043186 [PubMed: 17611206]

Huggett MT, Jermyn M, Gillams A, Illing R, Mosse S, Novelli M, … Pereira SP (2014). Phase I/II study of verteporfin photodynamic therapy in locally advanced pancreatic cancer. Br J Cancer, 110(7), 1698–1704. doi:10.1038/bjc.2014.95 [PubMed: 24569464]

Idris NM, Gnanasammandhan MK, Zhang J, Ho PC, Mahendran R, & Zhang Y (2012). In vivo photodynamic therapy using upconversion nanoparticles as remote-controlled nanotransducers. Nat Med, 18(10), 1580–1585. doi:10.1038/nm.2933 [PubMed: 22983397]

Josefsen LB, & Boyle RW (2008). Photodynamic therapy: novel third-generation photosensitizers one step closer? British Journal of Pharmacology, 154(1), 1–3. doi:10.1038/bjp.2008.98 [PubMed: 18362894]

Kamkaew A, Chen F, Zhan Y, Majewski RL, & Cai W (2016). Scintillating Nanoparticles as Energy Mediators for Enhanced Photodynamic Therapy. ACS Nano, 10(4), 3918–3935. doi:10.1021/acsnano.6b01401 [PubMed: 27043181]

Kashef N, Huang YY, & Hamblin MR (2017). Advances in antimicrobial photodynamic inactivation at the nanoscale. Nanophotonics, 6(5), 853–879. doi:10.1515/nanoph-2016-0189 [PubMed: 29226063]

Kerong D, Zhiyao H, Xiaoran D, Piaoping Y, Chunxia L, & Jun L (2015). Enhanced Antitumor Efficacy by 808 nm Laser-Induced Synergistic Photothermal and Photodynamic Therapy Based on a Indocyanine-Green-Attached W18O49 Nanostructure. Advanced Functional Materials, 25(47), 7280–7290. doi:doi:10.1002/adfm.201503046

Konan-Kouakou YN, Boch R, Gurny R, & Allemann E (2005). In vitro and in vivo activities of verteporfin-loaded nanoparticles. J Control Release, 103(1), 83–91. doi:10.1016/j.jconrel.2004.11.023 [PubMed: 15710502]

Leung SCH, Lo PC, Ng DKP, Liu WK, Fung KP, & Fong WP (2008). Photodynamic activity of BAM-SiPc, an unsymmetrical bisamino silicon(IV) phthalocyanine, in tumour-bearing nude mice. British Journal of Pharmacology, 154(1), 4–12. doi:10.1038/bjp.2008.82 [PubMed: 18332853]

Li M, Gao Y, Yuan Y, Wu Y, Song Z, Tang BZ, … Zheng QC (2017). One-Step Formulation of Targeted Aggregation-Induced Emission Dots for Image-Guided Photodynamic Therapy of Cholangiocarcinoma. ACS Nano, 11(4), 3922–3932. doi:10.1021/acsnano.7b00312 [PubMed: 28383899]

Li Y, Zhao Z, Zhang J, Kwok RTK, Xie S, Tang R, … Tang BZ (2018). A Bifunctional Aggregation-Induced Emission Luminogen for Monitoring and Killing of Multidrug-Resistant Bacteria. Advanced Functional Materials, 28(42), 1804632. doi:doi:10.1002/adfm.201804632

Lin J, Wang S, Huang P, Wang Z, Chen S, Niu G, … Nie Z (2013). Photosensitizer-loaded gold vesicles with strong plasmonic coupling effect for imaging-guided photothermal/photodynamic therapy. ACS Nano, 7(6), 5320–5329. doi:10.1021/nn4011686 [PubMed: 23721576]

Linlin L, Chuanfang C, Huiyu L, Changhui F, Longfei T, Shunhao W, … Hong L (2016). Multifunctional Carbon–Silica Nanocapsules with Gold Core for Synergistic Photothermal and Chemo-Cancer Therapy under the Guidance of Bimodal Imaging. Advanced Functional Materials, 26(24), 4252–4261. doi:doi:10.1002/adfm.201600985

Liu Y, Zhen W, Jin L, Zhang S, Sun G, Zhang T, … Zhang H (2018). All-in-One Theranostic Nanoagent with Enhanced Reactive Oxygen Species Generation and Modulating Tumor Microenvironment Ability for Effective Tumor Eradication. ACS Nano, 12(5), 4886–4893. doi:10.1021/acsnano.8b01893 [PubMed: 29727164]

Ma X, Qu Q, & Zhao Y (2015). Targeted delivery of 5-aminolevulinic acid by multifunctional hollow mesoporous silica nanoparticles for photodynamic skin cancer therapy. ACS Appl Mater Interfaces, 7(20), 10671–10676. doi:10.1021/acsami.5b03087 [PubMed: 25974979]

Malik Z, Ladan H, & Nitzan Y (1992). Photodynamic inactivation of Gram-negative bacteria: problems and possible solutions. J Photochem Photobiol B, 14(3), 262–266. [PubMed: 1432395]

Mellman I, Coukos G, & Dranoff G (2011). Cancer immunotherapy comes of age. Nature, 480(7378), 480–489. doi:10.1038/nature10673 [PubMed: 22193102]

Miller JD, Baron ED, Scull H, Hsia A, Berlin JC, McCormick T, … Oleinick NL (2007). Photodynamic therapy with the phthalocyanine photosensitizer Pc 4: the case experience with preclinical mechanistic and early clinical-translational studies. Toxicol Appl Pharmacol, 224(3), 290–299. doi:10.1016/j.taap.2007.01.025 [PubMed: 17397888]

Nauseef WM, & Borregaard N (2014). Neutrophils at work. Nat Immunol, 15(7), 602–611. doi: 10.1038/ni.2921 [PubMed: 24940954]

Nava HR, Allamaneni SS, Dougherty TJ, Cooper MT, Tan W, Wilding G, & Henderson BW (2011). PHOTODYNAMIC THERAPY (PDT) USING HPPH FOR THE TREATMENT OF PRECANCEROUS LESIONS ASSOCIATED WITH BARRETT'S ESOPHAGUS. Lasers Surg Med, 43(7), 705–712. doi:10.1002/lsm.21112 [PubMed: 22057498]

Noh I, Lee D, Kim H, Jeong CU, Lee Y, Ahn JO, … Kim YC (2018). Enhanced Photodynamic Cancer Treatment by Mitochondria-Targeting and Brominated Near-Infrared Fluorophores. Adv Sci (Weinh), 5(3), 1700481. doi:10.1002/advs.201700481 [PubMed: 29593951]

O'Connor AE, Gallagher WM, & Byrne AT (2009). Porphyrin and nonporphyrin photosensitizers in oncology: preclinical and clinical advances in photodynamic therapy. Photochem Photobiol, 85(5), 1053–1074. doi:10.1111/j.1751-1097.2009.00585.x [PubMed: 19682322]

Paszko E, Ehrhardt C, Senge MO, Kelleher DP, & Reynolds JV (2011). Nanodrug applications in photodynamic therapy. Photodiagnosis and Photodynamic Therapy, 8(1), 14–29. doi:10.1016/j.pdpdt.2010.12.001 [PubMed: 21333931]

Reidy K, Campanile C, Muff R, Born W, & Fuchs B (2012). mTHPC-mediated photodynamic therapy is effective in the metastatic human 143B osteosarcoma cells. Photochem Photobiol, 88(3), 721–727. doi:10.1111/j.1751-1097.2012.01096.x [PubMed: 22268498]

Senge MO (2012). mTHPC – A drug on its way from second to third generation photosensitizer? Photodiagnosis and Photodynamic Therapy, 9(2), 170–179. doi:10.1016/j.pdpdt.2011.10.001 [PubMed: 22594988]

Shafirstein G, Bäumler W, Hennings LJ, Siegel ER, Friedman R, Moreno MA, … Griffin RJ (2012). Indocyanine Green Enhanced Near Infrared Laser Treatment of Murine Mammary Carcinoma. Int J Cancer, 130(5), 1208–1215. doi:10.1002/ijc.26126 [PubMed: 21484791]

Shu X, Lev-Ram V, Deerinck TJ, Qi Y, Ramko EB, Davidson MW, … Tsien RY (2011). A genetically encoded tag for correlated light and electron microscopy of intact cells, tissues, and organisms. PLoS Biol, 9(4), e1001041. doi:10.1371/journal.pbio.1001041 [PubMed: 21483721]

Simone CB 2nd, Friedberg JS, Glatstein E, Stevenson JP, Sterman DH, Hahn SM, & Cengel KA (2012). Photodynamic therapy for the treatment of non-small cell lung cancer. J Thorac Dis, 4(1), 63–75. doi:10.3978/j.issn.2072-1439.2011.11.05 [PubMed: 22295169]

Song C, Yang C, Wang F, Ding D, Gao Y, Guo W, … Guo C (2017). MoS2-Based multipurpose theranostic nanoplatform: realizing dual-imaging-guided combination phototherapy to eliminate solid tumor via a liquefaction necrosis process. Journal of Materials Chemistry B, 5(45), 9015–9024. doi:10.1039/C7TB02648J

Spellberg B, Bartlett JG, & Gilbert DN (2013). The future of antibiotics and resistance. N Engl J Med, 368(4), 299–302. doi:10.1056/NEJMp1215093 [PubMed: 23343059]

Starkey JR, Rebane AK, Drobizhev MA, Meng F, Gong A, Elliott A, … Spangler CW (2008). New two-photon activated photodynamic therapy sensitizers induce xenograft tumor regressions after near-IR laser treatment through the body of the host mouse. Clin Cancer Res, 14(20), 6564–6573. doi:10.1158/1078-0432.ccr-07-4162 [PubMed: 18927297]

Tao Y, Ling L, Yibin D, Zhengqing G, Guobing Z, Zhishen G, … Huabing C (2017). Ultrastable Near-Infrared Conjugated-Polymer Nanoparticles for Dually Photoactive Tumor Inhibition. Advanced Materials, 29(31), 1700487. doi:doi:10.1002/adma.201700487

Taratula O, Schumann C, Naleway MA, Pang AJ, Chon KJ, & Taratula O (2013). A Multifunctional Theranostic Platform Based on Phthalocyanine-Loaded Dendrimer for Image-Guided Drug Delivery and Photodynamic Therapy. Molecular Pharmaceutics, 10(10), 3946–3958. doi:10.1021/mp400397t [PubMed: 24020847]

Taylor PW, Stapleton PD, & Paul Luzio J (2002). New ways to treat bacterial infections. Drug Discov Today, 7(21), 1086–1091. doi:10.1016/S1359-6446(02)02498-4 [PubMed: 12546840]

Torchilin VP (2014). Multifunctional, stimuli-sensitive nanoparticulate systems for drug delivery. Nat Rev Drug Discov, 13(11), 813–827. doi:10.1038/nrd4333 [PubMed: 25287120]

Tour O, Meijer RM, Zacharias DA, Adams SR, & Tsien RY (2003). Genetically targeted chromophore-assisted light inactivation. Nat Biotechnol, 21(12), 1505–1508. doi:10.1038/nbt914 [PubMed: 14625562]

Triesscheijn M, Baas P, Schellens JH, & Stewart FA (2006). Photodynamic therapy in oncology. Oncologist, 11(9), 1034–1044. doi:10.1634/theoncologist.11-9-1034 [PubMed: 17030646]

Tu H-L, Lin Y-S, Lin H-Y, Hung Y, Lo L-W, Chen Y-F, & Mou C-Y (2009). In vitro Studies of Functionalized Mesoporous Silica Nanoparticles for Photodynamic Therapy. Advanced Materials, 21(2), 172–177. doi:doi:10.1002/adma.200800548

Vankayala R, & Hwang KC (2018). Near-Infrared-Light-Activatable Nanomaterial-Mediated Phototheranostic Nanomedicines: An Emerging Paradigm for Cancer Treatment. Adv Mater, 30(23), e1706320. doi:10.1002/adma.201706320 [PubMed: 29577458]

Wainwright M, Maisch T, Nonell S, Plaetzer K, Almeida A, Tegos GP, & Hamblin MR (2017). Photoantimicrobials-are we afraid of the light? Lancet Infect Dis, 17(2), e49–e55. doi:10.1016/s1473-3099(16)30268-7 [PubMed: 27884621]

Wallace DC (2012). Mitochondria and cancer. Nat Rev Cancer, 12(10), 685–698. doi:10.1038/nrc3365 [PubMed: 23001348]

Wang AZ, Langer R, & Farokhzad OC (2012). Nanoparticle delivery of cancer drugs. Annu Rev Med, 63, 185–198. doi:10.1146/annurev-med-040210-162544 [PubMed: 21888516]

Wang S, Gao J, Li M, Wang L, & Wang Z (2018). A facile approach for development of a vaccine made of bacterial double-layered membrane vesicles (DMVs). Biomaterials, 187, 28–38. doi:10.1016/j.biomaterials.2018.09.042 [PubMed: 30292939]

Wang S, Gao J, & Wang Z (2018). Outer membrane vesicles for vaccination and targeted drug delivery. Wiley Interdiscip Rev Nanomed Nanobiotechnol, e1523. doi:10.1002/wnan.1523 [PubMed: 29701017]

Wang X, Peralta S, & Moraes CT (2013). Mitochondrial alterations during carcinogenesis: a review of metabolic transformation and targets for anticancer treatments. Adv Cancer Res, 119, 127–160. doi:10.1016/b978-0-12-407190-2.00004-6 [PubMed: 23870511]

Wang Y, Wang Y, Wang Y, Murray CK, Hamblin MR, Hooper DC, & Dai T (2017). Antimicrobial blue light inactivation of pathogenic microbes: State of the art. Drug Resist Updat, 33–35, 1–22. doi:10.1016/j.drup.2017.10.002

Wang Z, Li J, Cho J, & Malik AB (2014). Prevention of vascular inflammation by nanoparticle targeting of adherent neutrophils. Nat Nanotechnol, 9(3), 204–210. doi:10.1038/nnano.2014.17 [PubMed: 24561355]

Wang Z, & Malik AB (2013). Nanoparticles squeezing across the blood-endothelial barrier via caveolae. Ther Deliv, 4(2), 131–133. doi:10.4155/tde.12.140 [PubMed: 23343150]

Wang Z, & Rothberg LJ (2007). Structure and dynamics of single conjugated polymer chromophores by surface-enhanced Raman spectroscopy. ACS Nano, 1(4), 299–306. doi:10.1021/nn700213t [PubMed: 19206680]

Wang Z, Tiruppathi C, Cho J, Minshall RD, & Malik AB (2011). Delivery of nanoparticle: complexed drugs across the vascular endothelial barrier via caveolae. IUBMB Life, 63(8), 659–667. doi:10.1002/iub.485 [PubMed: 21766412]

Wang Z, Tiruppathi C, Minshall RD, & Malik AB (2009). Size and dynamics of caveolae studied using nanoparticles in living endothelial cells. ACS Nano, 3(12), 4110–4116. doi:10.1021/nn9012274 [PubMed: 19919048]

Webber MA, & Piddock LJV (2003). The importance of efflux pumps in bacterial antibiotic resistance. Journal of Antimicrobial Chemotherapy, 51(1), 9–11. doi:10.1093/jac/dkg050 [PubMed: 12493781]

Westberg M, Holmegaard L, Pimenta FM, Etzerodt M, & Ogilby PR (2015). Rational design of an efficient, genetically encodable, protein-encased singlet oxygen photosensitizer. J Am Chem Soc, 137(4), 1632–1642. doi:10.1021/ja511940j [PubMed: 25575190]

Wöhrle D, Shopova M, Müller S, Milev AD, Mantareva VN, & Krastev KK (1993). Liposome-delivered Zn(II)-2,3-naphthalocyanines as potential sensitizers for PDT: synthesis, photochemical, pharmacokinetic and phototherapeutic studies. Journal of Photochemistry and Photobiology B: Biology, 21(2), 155–165. doi:10.1016/1011-1344(93)80178-C

Xie J, Pan X, Wang M, Yao L, Liang X, Ma J, … Mi L (2016). Targeting and Photodynamic Killing of Cancer Cell by Nitrogen-Doped Titanium Dioxide Coupled with Folic Acid. Nanomaterials (Basel), 6(6). doi:10.3390/nano6060113

Xing R, Liu K, Jiao T, Zhang N, Ma K, Zhang R, … Yan X (2016). An Injectable Self-Assembling Collagen-Gold Hybrid Hydrogel for Combinatorial Antitumor Photothermal/Photodynamic Therapy. Adv Mater, 28(19), 3669–3676. doi:10.1002/adma.201600284 [PubMed: 26991248]

Yan Y, Bjornmalm M, & Caruso F (2013). Particle carriers for combating multidrug-resistant cancer. ACS Nano, 7(11), 9512–9517. doi:10.1021/nn405632s [PubMed: 24215340]

Yano T, Hatogai K, Morimoto H, Yoda Y, & Kaneko K (2014). Photodynamic therapy for esophageal cancer. Ann Transl Med, 2(3), 29. doi:10.3978/j.issn.2305-5839.2014.03.01 [PubMed: 25333005]

Yogo T, Urano Y, Ishitsuka Y, Maniwa F, & Nagano T (2005). Highly efficient and photostable photosensitizer based on BODIPY chromophore. J Am Chem Soc, 127(35), 12162–12163. doi: 10.1021/ja0528533 [PubMed: 16131160]

Yurt F, Ince M, Colak SG, Ocakoglu K, Er O, Soylu HM, … Kurt CC (2017). Investigation of in vitro PDT activities of zinc phthalocyanine immobilised TiO2 nanoparticles. Int J Pharm, 524(1–2), 467–474. doi:10.1016/j.ijpharm.2017.03.050 [PubMed: 28365390]

Zhang C, Bu W, Ni D, Zhang S, Li Q, Yao Z, … Shi J (2016). Synthesis of Iron Nanometallic Glasses and Their Application in Cancer Therapy by a Localized Fenton Reaction. Angew Chem Int Ed Engl, 55(6), 2101–2106. doi:10.1002/anie.201510031 [PubMed: 26836344]

Zhang CY, Gao J, & Wang Z (2018). Bioresponsive Nanoparticles Targeted to Infectious Microenvironments for Sepsis Management. Adv Mater, 30(43), e1803618. doi:10.1002/adma.201803618 [PubMed: 30203430]

Zhang J, Yang C, Zhang R, Chen R, Zhang Z, Zhang W, … Lee CS (2017). Biocompatible D-A Semiconducting Polymer Nanoparticle with Light-Harvesting Unit for Highly Effective Photoacoustic Imaging Guided Photothermal Therapy. Adv Funct Mater, 27(13). doi:10.1002/adfm.201605094

Zhang S, Guo W, Wei J, Li C, Liang X-J, & Yin M (2017). Terrylenediimide-Based Intrinsic Theranostic Nanomedicines with High Photothermal Conversion Efficiency for Photoacoustic Imaging-Guided Cancer Therapy. ACS Nano, 11(4), 3797–3805. doi:10.1021/acsnano.6b08720 [PubMed: 28301720]

Zhang Y, Wang Z, Ng MK, & Rothberg LJ (2007). Conformational reorganization and solvation dynamics of dendritic oligothiophenes. J Phys Chem B, 111(46), 13211–13216. doi:10.1021/jp077564a [PubMed: 17973424]

Zhao Z, Han Y, Lin C, Hu D, Wang F, Chen X, …Zheng N (2012). Multifunctional core-shell upconverting nanoparticles for imaging and photodynamic therapy of liver cancer cells. Chem Asian J, 7(4), 830–837. doi:10.1002/asia.201100879 [PubMed: 22279027]

Zhou L, Zhou L, Wei S, Ge X, Zhou J, Jiang H, … Shen J (2014). Combination of chemotherapy and photodynamic therapy using graphene oxide as drug delivery system. Journal of Photochemistry and Photobiology B: Biology, 135, 7–16. doi:10.1016/j.jphotobiol.2014.04.010

Zhou Z, Song J, Nie L, & Chen X (2016). Reactive oxygen species generating systems meeting challenges of photodynamic cancer therapy. Chem Soc Rev, 45(23), 6597–6626. doi:10.1039/c6cs00271d [PubMed: 27722328]

Zhou Z, Song J, Nie L, & Chen X (2016). Reactive Oxygen Species Generating Systems Meeting Challenges of Photodynamic Cancer Therapy. Chem Soc Rev, 45(23), 6597–6626. doi:10.1039/c6cs00271d [PubMed: 27722328]

Zhu H, Fang Y, Miao Q, Qi X, Ding D, Chen P, & Pu K (2017). Regulating Near-Infrared Photodynamic Properties of Semiconducting Polymer Nanotheranostics for Optimized Cancer Therapy. ACS Nano, 11(9), 8998–9009. doi:10.1021/acsnano.7b03507 [PubMed: 28841279]

Zou Z, Chang H, Li H, & Wang S (2017). Induction of reactive oxygen species: an emerging approach for cancer therapy. Apoptosis, 22(11), 1321–1335. doi:10.1007/s10495-017-1424-9 [PubMed: 28936716]

Zuluaga MF, & Lange N (2008). Combination of photodynamic therapy with anti-cancer agents. Curr Med Chem, 15(17), 1655–1673. [PubMed: 18673216]

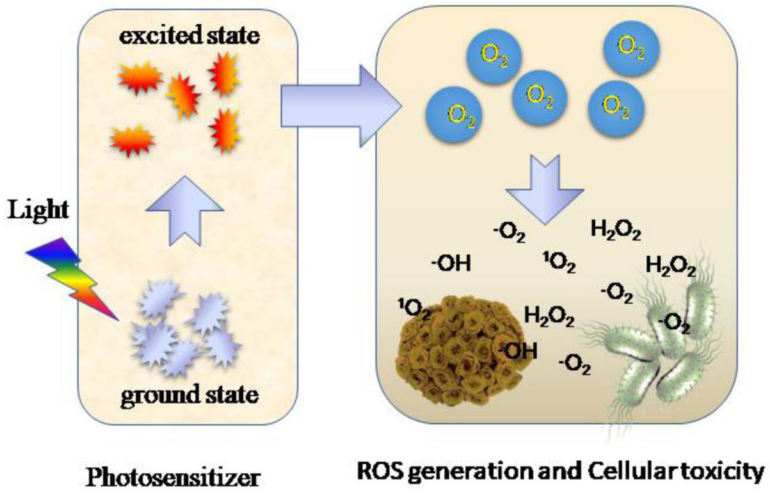

Figure 1.
Schematic illustration of the photochemical reactions in PDT.

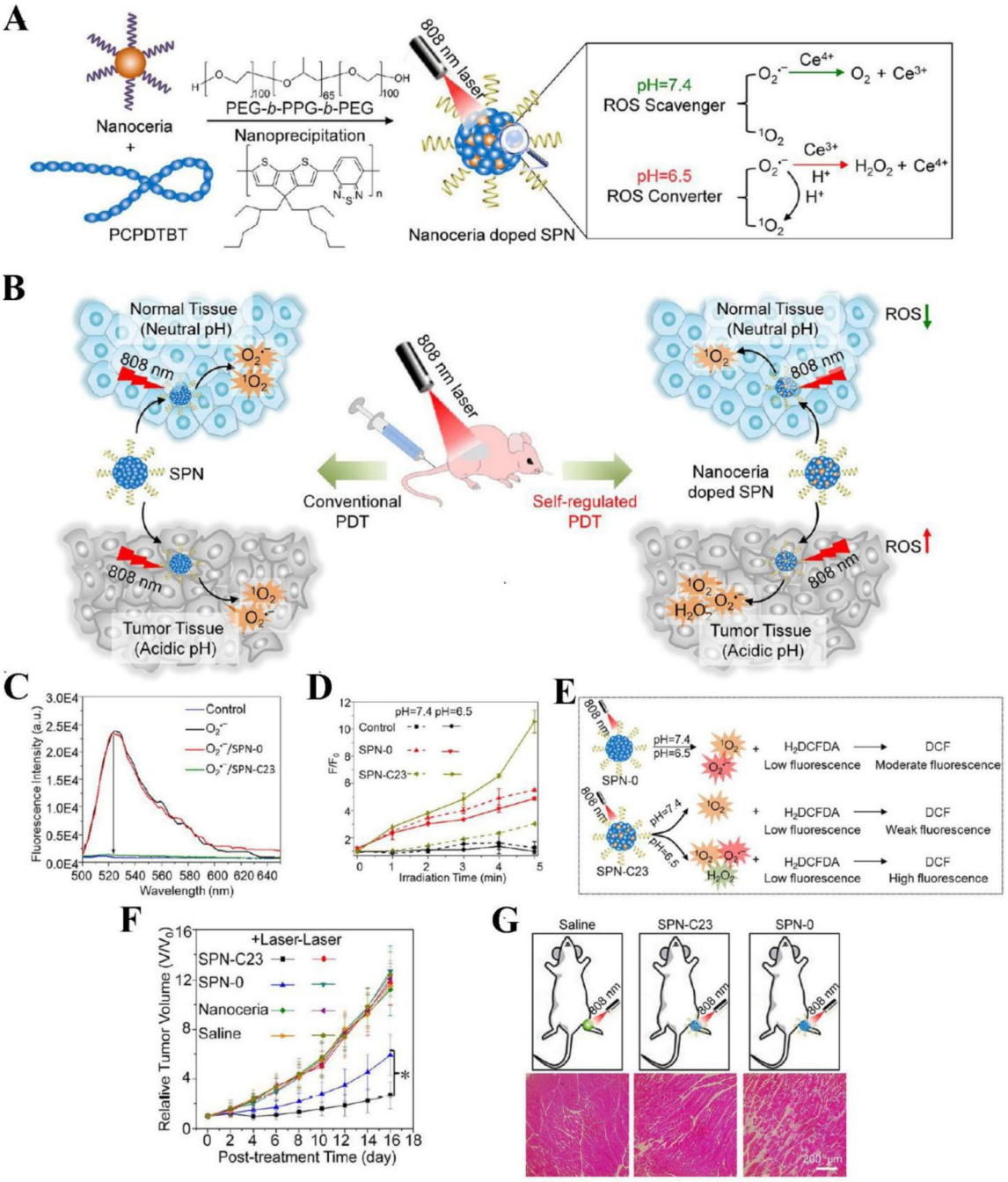

Figure 2.

Schematics show the components of SPNs doped with nanoceria and the concept of controllable photodynamic capacities of SPNs that are dependent on tissue microenvironments (A), and the differences between conventional PDT and self-regulated PDT when nanoceria are doped in SPNs (B). (C) *In vitro* studies show the capabilities of ROS scavenging by SPNs. Fluorescence intensities of ROS indicator were measured after addition of SPNs doped with different amount of nanoceria. (D) *In vitro* ROS generation from SPNs. The fluorescence changes of ROS indicator mixed with SPN-0 or SPN-C23 in

different pH conditions irradiated with laser at 808 nm (0.44 W/cm^2) as a function of irradiation time. (E) The graph illustrates the different responses of ROS in SPN-0 or SPN-C23 after irradiated with NIR laser and ROS responses were measured by H_2DCFDA. (F) Tumor growth after mice were treated with different drug formulations. (G) Histological H&E staining of mouse muscles 24 h after the different treatments irradiated with NIR laser for 5 min. Reproduced with permission (Zhu et al., 2017). Copyright 2017, American Chemical Society.

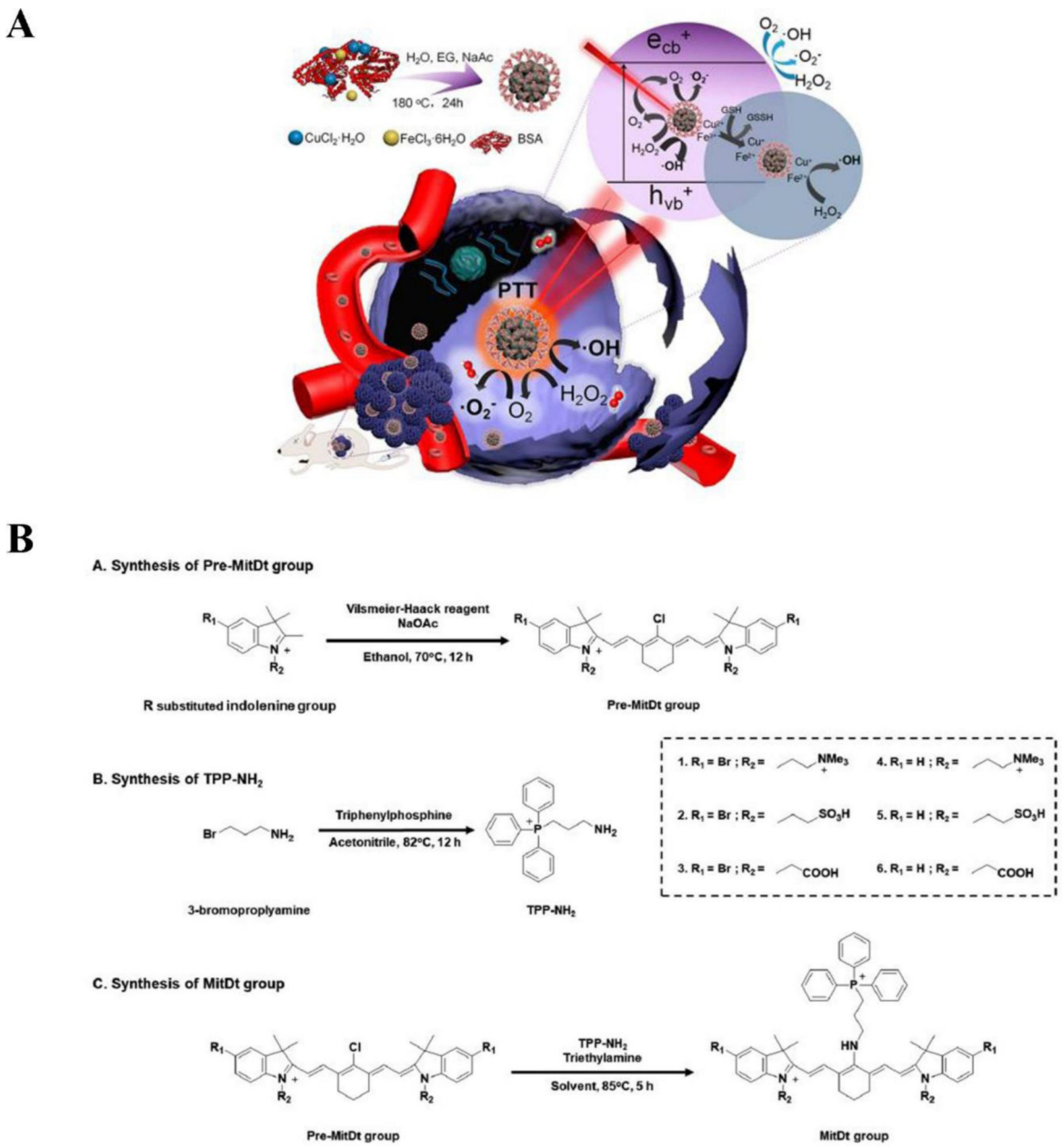

Figure 3.

(A) Synthetic process of CFNs and their therapeutic mechanism. Reproduced with permission (Liu et al., 2018). Copyright 2018, American Chemical Society. (B) Structure and synthetic processes for MitDt groups. Reproduced with permission (Noh et al., 2018). Copyright 2017, Wiley-VCH.

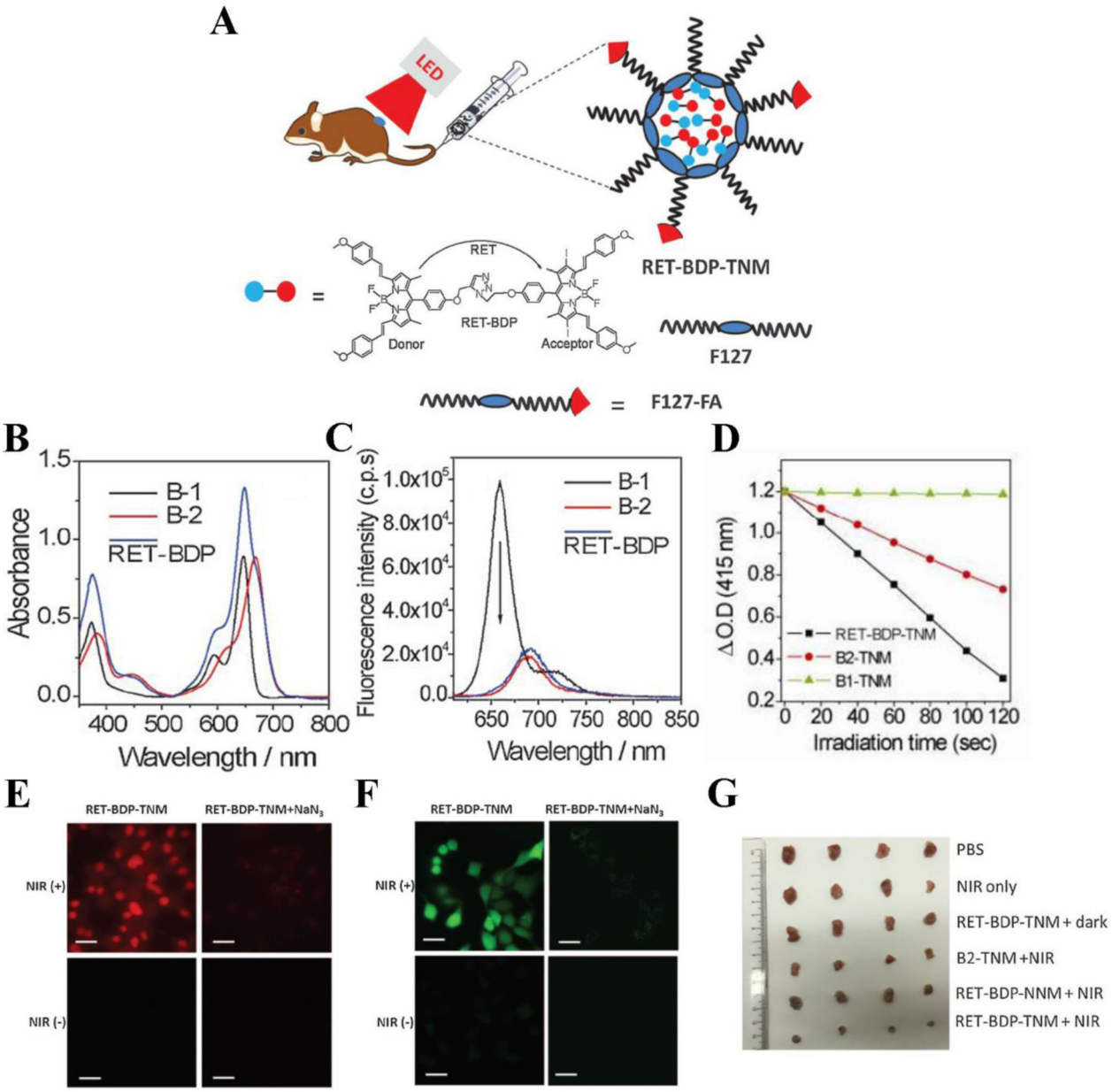

Figure 4.

(A) Concept and structure of RET-BDP-TNM. (B) Absorption spectra of donor moiety B-1, acceptor moiety B-2, and RET-BDP. (C) Fluorescence emission spectra of donor moiety B-1, acceptor moiety B-2, and RET-BDP upon excitation with 610 nm light. (D) The change of DPBF optical density *vs* irradiation time for mixtures of DPBF with RET-BDP-TNM, B1-TNM, and B2-TNM respectively, upon excitation with 645 nm light (10 mW cm^{-2}). (E) PDT effect of RET-BDP-TNM in HeLa cells with PI staining for dead cells observed by confocal fluorescence microscopy. (F) ROS generation of RET-BDP-TNM in HeLa cells measured by DCFH-DA. (G) digital pictures of 4T1 tumors with different treatments. Scale bar represents 30 μm. Reproduced with permission (L. Huang et al., 2017). Copyright 2017, John Wiley and Sons.

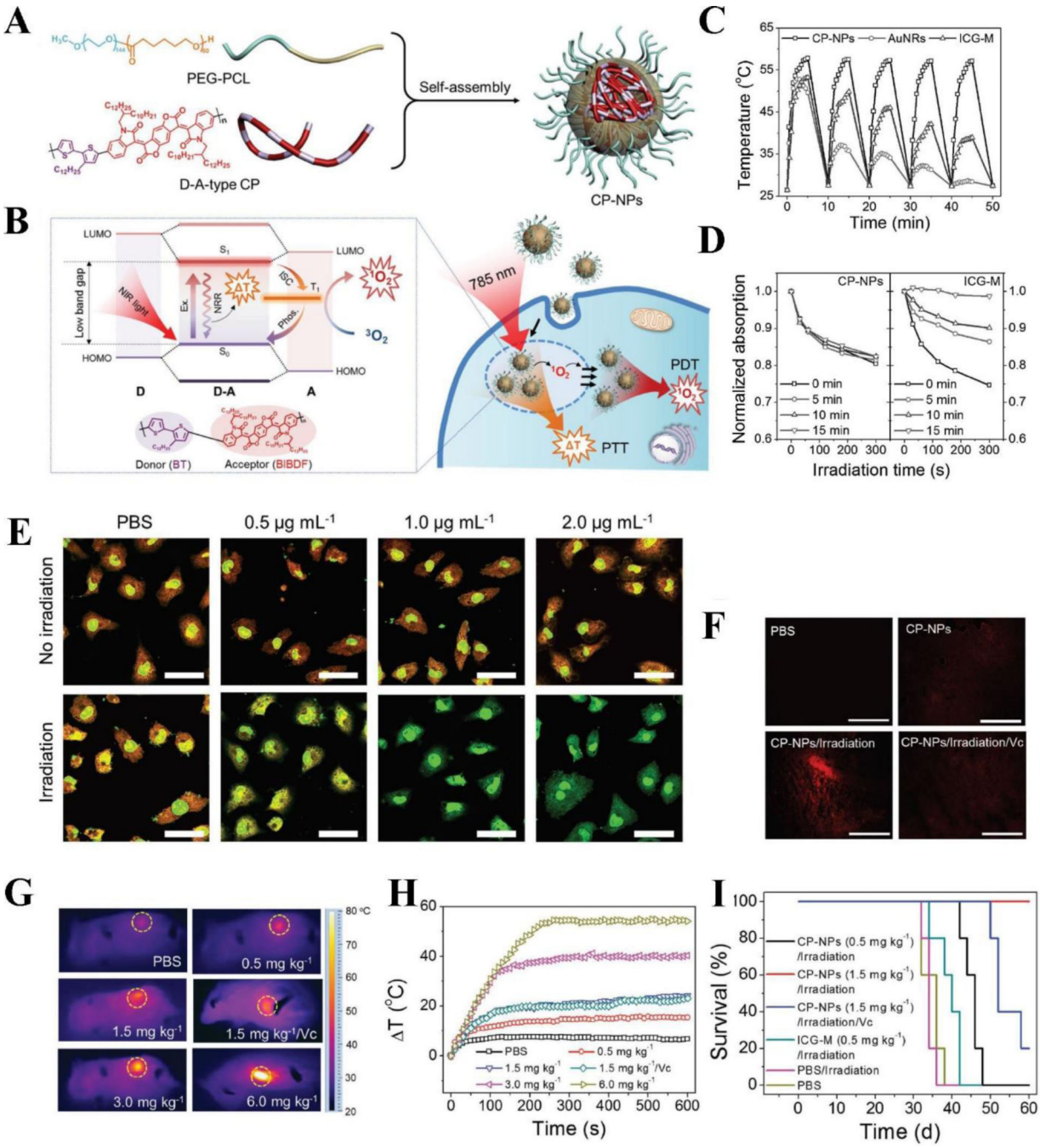

Figure 5.

(A) Structure of D-A-type CP-NPs. (B) Photophysical mechanism for dual PTT/PDT in cancer treatment using D-A-type CP-NPs. (C) The plot of temperature changes in CP-NPs, AuNRs, and ICG-M during repeatable irradiation/cooling cycles. (D) The plot of ROS production of CP-NPs and ICG-M during different irradiation time (λ_{ex} = 785 nm, 1.5 W cm^{-2}). (E) $^1O_2$ generation in acridine orange (AO) stained 4T1 tumor cells treated with different concentrations of CP-NPs with or without irradiation observed using confocal microscopy (Scale bar represents 20 μm). (F) ROS generation in tumor of the mice stained

by DHE under irradiation with different treatments (scale bar represents 100 μm). (G) Temperature elevation in tumor area (yellow circle) of the mice treated with different doses of CP-NPs under irradiation. (H) Quantification of temperature elevation at tumor area of the mice treated with different doses of CP-NPs under irradiation. (I) 4T1 tumor-bearing mice survival rate with different treatments. Reproduced with permission (Tao et al., 2017). Copyright 2017, John Wiley and Sons.

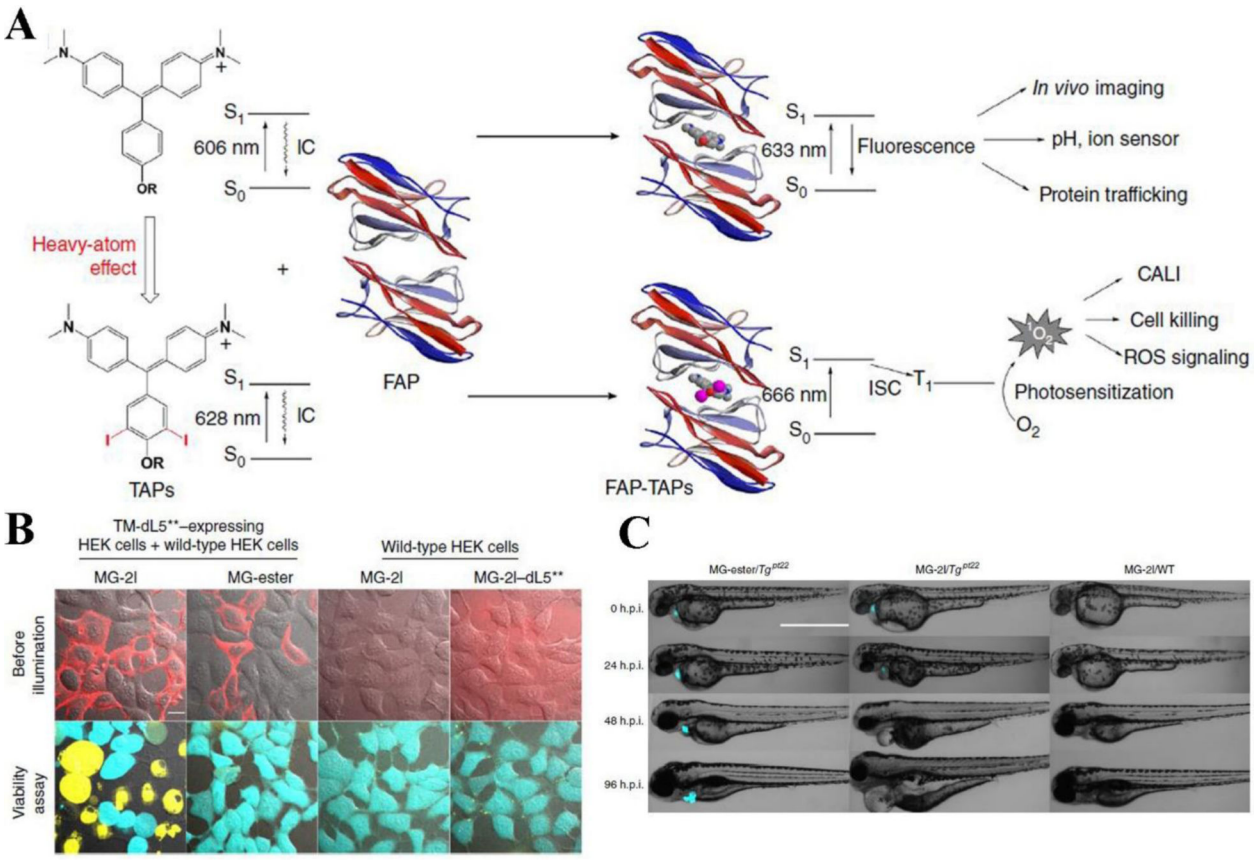

Figure 6.

(A) Schematic illustration of photosensitizing effect induced by FAP-TAPs. (B) Cellular photoablation of FAP-TAPs on HEK cells expressing TM-dL5** and wild-type HEK293 cells. Fluorescently labeled HEK cells were treated with MG-2I, MG-ester and non-targeted MG-2I/ dL5** in the concentration of 400 nM for 30 min before illuminated with light (λ_{ex} = 640 nm, 0.76 W cm^{-2}, 1 min). 30 minutes later, live/dead cell viability was assayed. Scale bar represents 10 μm. (C) FAP-TAPs demonstrate the damage to cardiac function and phenotype development of adult zebrafish expressed dL5** in the heart, photos show the change in development of phenotype from 0 h.p.i. to 96 h.p.i. in wild-type and dL5** expressed zebrafish with different treatments. scale bar represents 1000 μm. Reproduced with permission (J. He et al., 2016). Copyright 2016, Springer Nature.

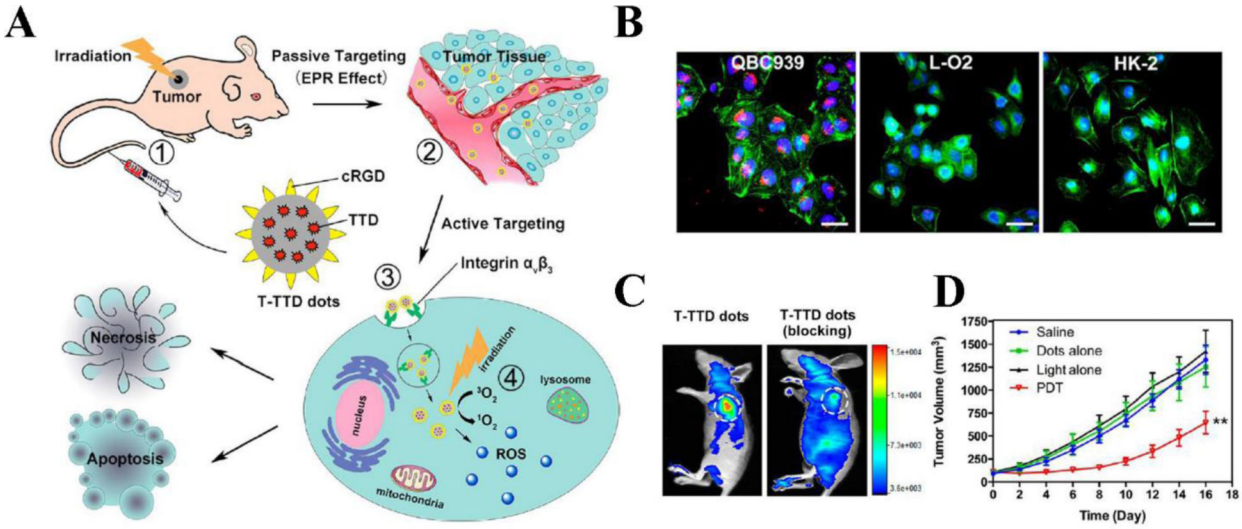

Figure 7.

(A) Hypothesis depiction of T-TTD dots accumulation in tumor through passive and active targeting, and tumor ablation *via* PDT. (B) Fluorescent signal of T-TTD dots (red) observed in QBC939 cells, while weak fluorescence of T-TTD dots in L-O2, and HK-2 cells after incubation with T-TTD dots (5 μg/mL) for 4 h. Nuclei is labeled as blue and cytoskeleton is labeled as green. Scale bar represents 50 μm. (C) *In vivo* targeting ability of T-TTD dots to tumor, after blocking the receptors, the tumor uptake of dots is significantly inhibited. (D) Tumor volume curve of mice with different treatments. Data represent mean ± SD; **p < 0.01. Reproduced with permission (M. Li et al., 2017). Copyright 2017, American Chemical Society.

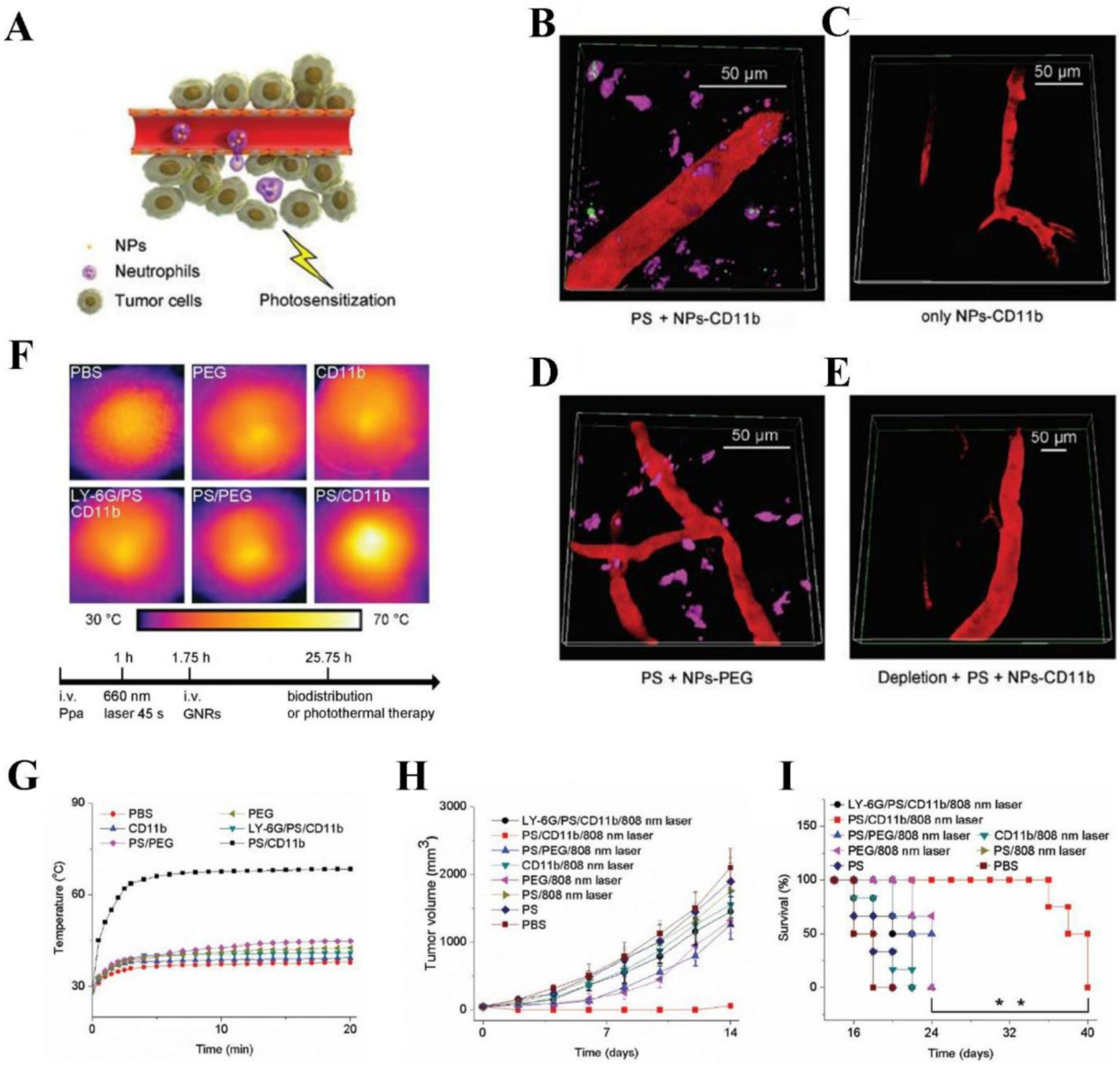

Figure 8.

(A) Hypothesis illustration of NPs taken up by activated neutrophils to inflamed tumors induced by photosensitization. (B), (C), (D), (E) Mouse tumors with different treatments observed using intravital microscopy. PS represents photosensitization (intravenous injection of Ppa followed by tumors irradiated with 660nm laser). (F) Images of hyperthermia in mouse tumors with different treatments after photosensitization. (G) Temperature change of tumor versus irradiation time during photosensitization. (H) Tumor volume and (I) survival rate of the tumor-bearing mice with different treatments. Data represent mean ± standard deviation, $^{**}p < 0.01$. Reproduced with permission (Chu et al., 2017). Copyright 2017, John Wiley and Sons.

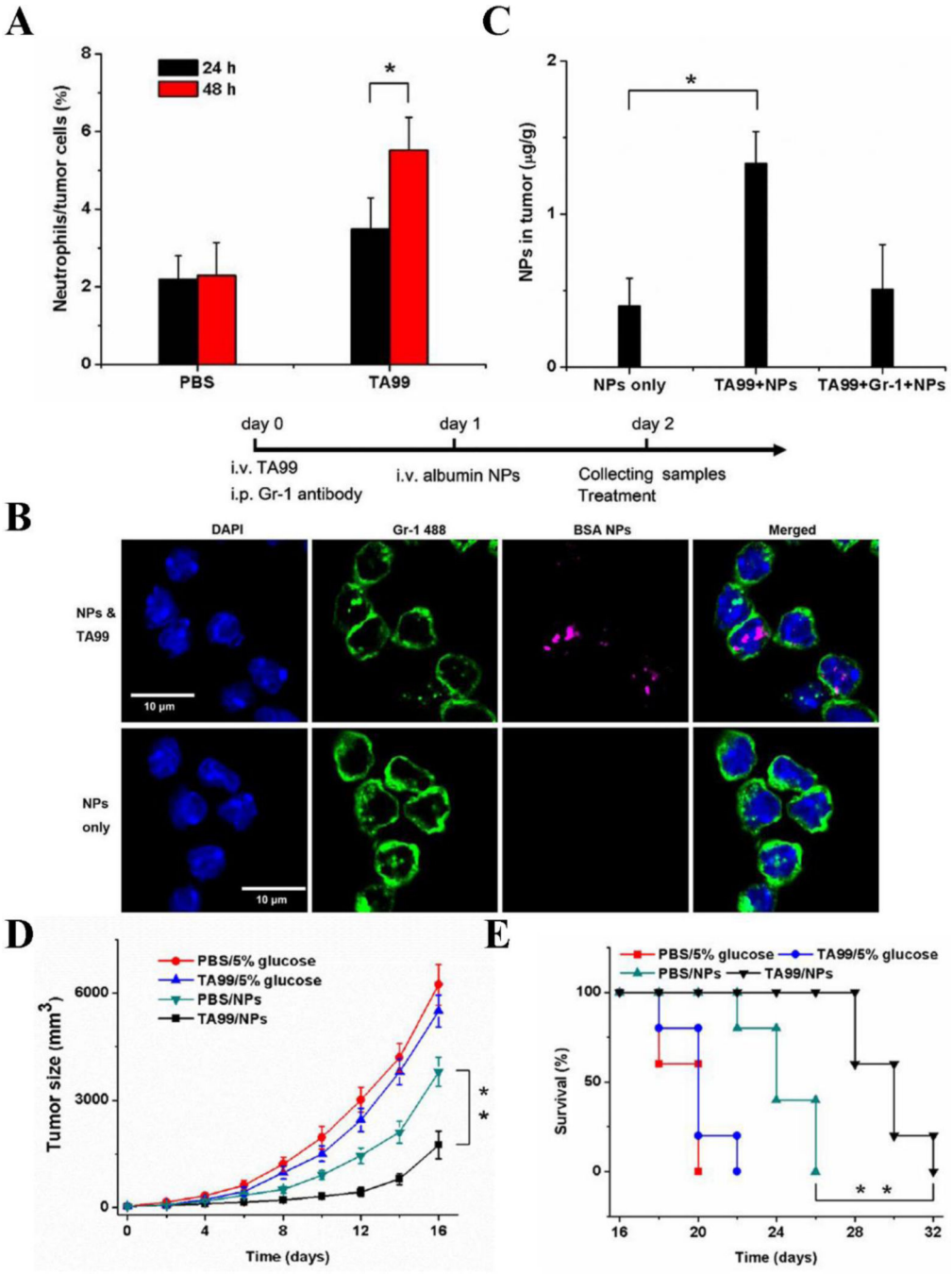

Figure 9.

(A) Contents of neutrophils in tumor tissue 24 h or 48 h after injection of PBS and TA99. Tumor samples were subjected to single cell suspension after treatments and measured by flow cytometry. (B) Neutrophils (green) uptake of albumin nanoparticles (red) with or without TA99 observed using fluorescence confocal microscopy. Nucleus was marked by DAPI (blue). (C) Contents of BSA NPs in tumor tissue with different indicated treatments, TA99 obviously increases the contents of albumin NPs in tumor tissue. Anti-Gr-1 antibody applied for depleting neutrophils. The measurements of (D) tumor volume, (E) survival rates

of bearing melanoma mice illuminated with 660 nm laser under different treatments. Treatments include injection of vehicles, TA99, Ppa-loaded NPs, or both of TA99 and Ppa-loaded NPs, the effectiveness of PDT mediated cancer therapy has been confirmed, *$p < 0.05$, **$p < 0.01$. Reproduced with permission (Chu et al., 2016). Copyright 2016, John Wiley and Sons.

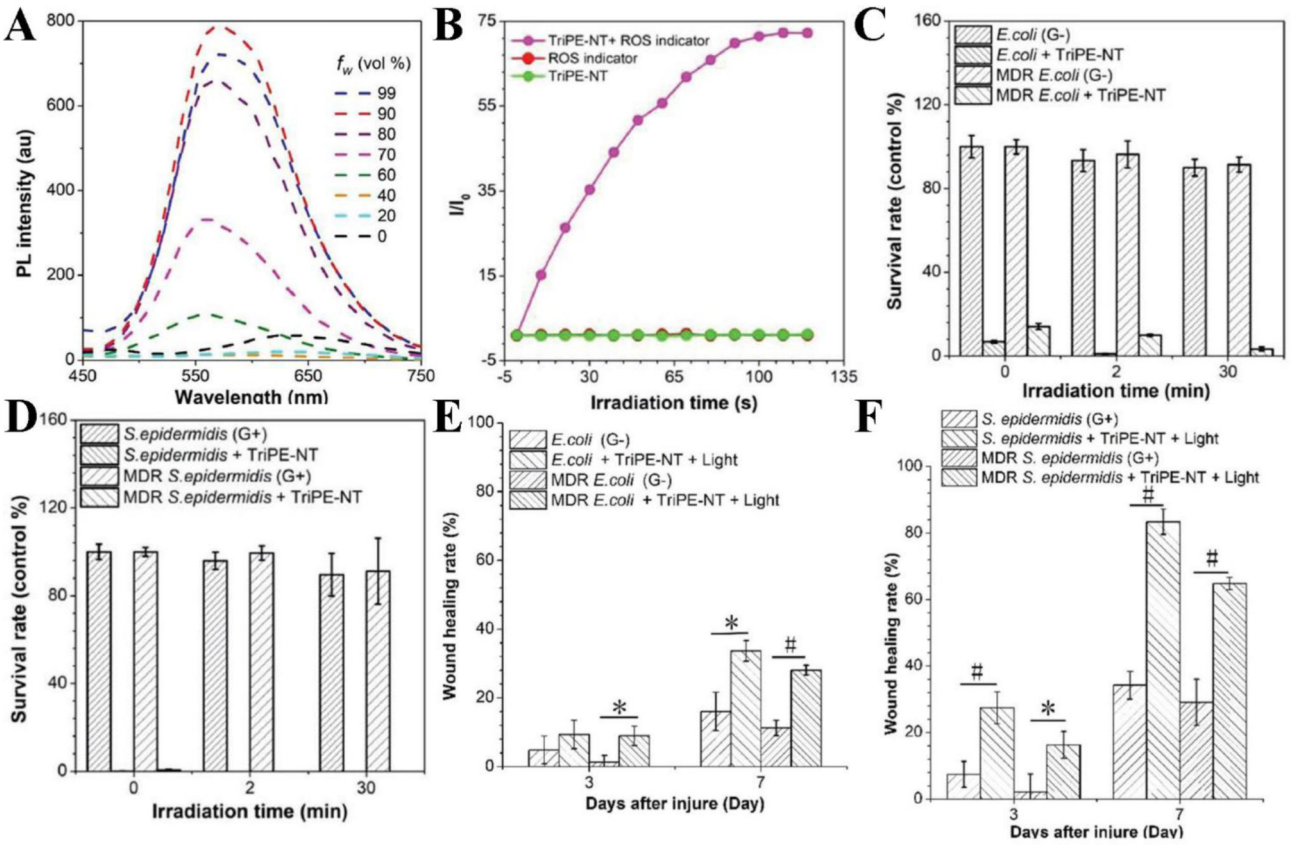

Figure 10.

(A) Measurements of PL intensity of TriPE-NT in THF with different proportion of water. (B) Plotting of fluorescence intensity of DCFH with or without presence of TriPE-NT irradiated with white light. (C) Survival rates of *E. coli* wild type and MDR bacteria under different white light irradiation time treated with or without TriPE-NT. (D) Survival rates of *S. epidermidis* wild type and MDR bacteria under different white light irradiation time treated with or without TriPE-NT. (E) The percentage of *E. coli* wild type and MDR bacteria-infected wound area 3 or 7 days after surgery, with or without treatment of TriPE-NT. (F) The percentage of *S. epidermidis* wild type and MDR bacteria-infected wound area 3 or 7 days after surgery, with or without treatment of TriPE-NT and irradiation. (#$p < 0.001$, $0.001 < *p < 0.05$). Reproduced with permission (Y. Li et al., 2018). Copyright 2018, John Wiley and Sons.

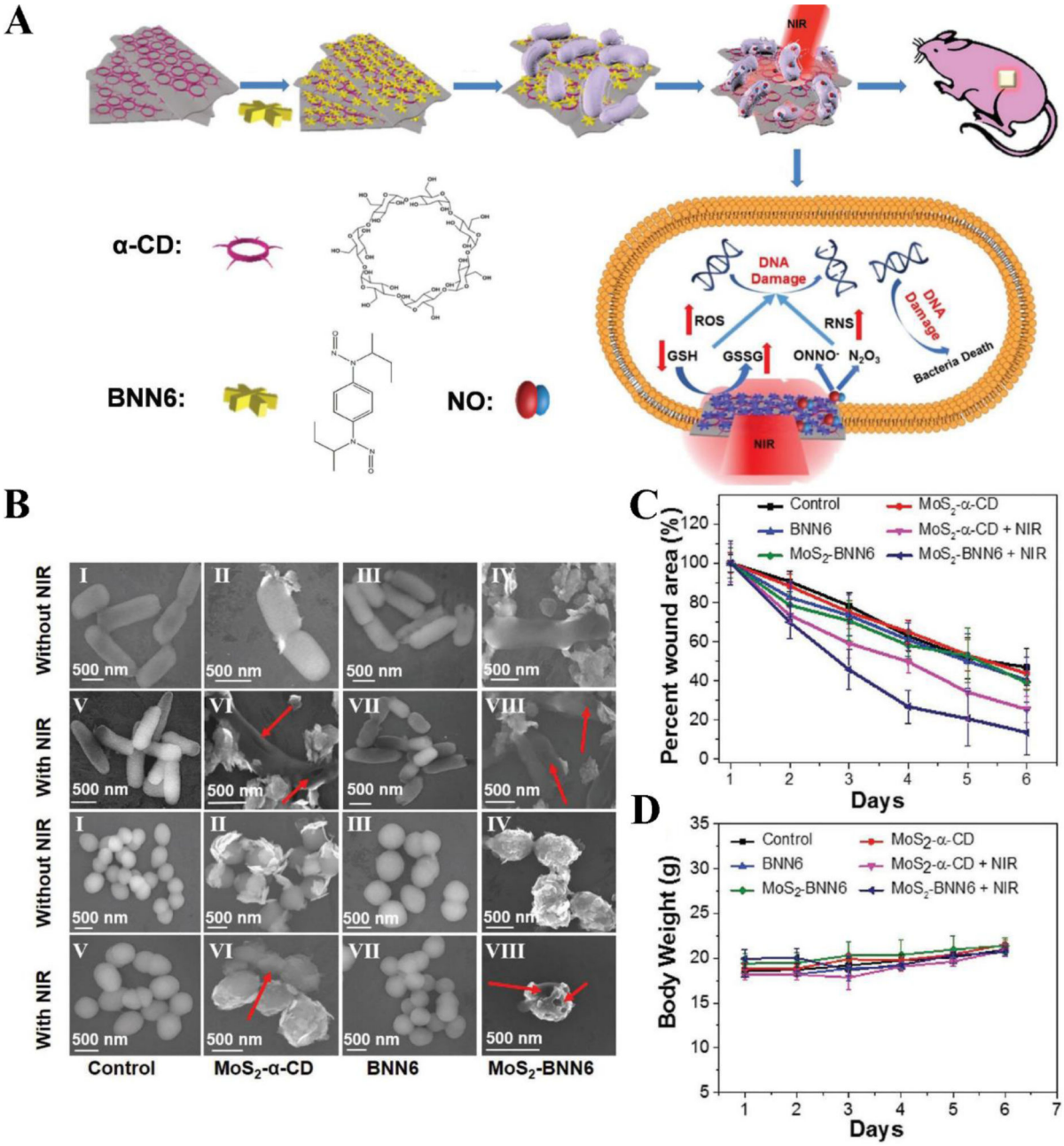

Figure 11.

(A) Synthesis process of MoS_2-BNN6 and PTT/NO synergistic treatments for killing bacteria. (B) Field Emission Scanning Electron Microscopy (FE-SEM) photos of Amp^r *E.coli* (first and second lines) and *E. faecalis* (third and fourth lines) with different indicated treatments. Red arrows indicate the broken sites of bacteria. (C) Wound area changes of mice with indicated treatments. (D) Body weight change of mice with different treatments. Reproduced with permission (Q. Gao et al., 2018). Copyright 2018, John Wiley and Sons.

Table 1.

Summary of representative PSs used in PDT.

Type	Class	Representative PSs	Absorption wavelength	Ref.
First generation of organic PSs	Porphyrin derivatives	Photofrin (HPD), HP, PpIX	630 nm	(M. C. DeRosa & Crutchley, 2002; Ethirajan, Chen, Joshi, & Pandey, 2011; Ma, Qu, & Zhao, 2015; O'Connor, Gallagher, & Byrne, 2009; Tu et al., 2009)
Second generation of organic PSs	Pyropheophorbide-a	Photochlor	665 nm	(Bellnier et al., 2006; Nava et al., 2011)
	Phthalocyanine derivatives	ZnPC, SPCD, AlC_4Pc, Pc4	660 nm	(Miller et al., 2007; Taratula et al., 2013; Yurt et al., 2017; Zhao et al., 2012)
	Chlorine derivatives	Ce6, m-THPC	660 nm	(Ai et al., 2015; Reidy, Campanile, Muff, Born, & Fuchs, 2012; Senge, 2012)
	Benzoporphyrin derivatives	Visudyne	690 nm	(Huggett et al., 2014)
	NIR-absorbing PSs	ICG, Cypate, Tookad, Naphthalocyanines	700–800 nm	(Guo et al., 2014; Z. Huang et al., 2007; Shafirstein et al., 2012; Wöhrle et al., 1993)
Inorganic PSs		TiO_2, CdSe, ZnO, C_{60}, etc.	UV, NIR	(Ancona et al., 2018; S. J. He et al., 2016; Y. Y. Huang et al., 2014; Xie et al., 2016)
Third generation of PSs	PSs bearing targeting moieties	PS bioconjugates	UV, NIR	(Q. Chen et al., 2016; Du et al., 2017; Han, Park, Park, & Na, 2016; Idris et al., 2012; Noh et al., 2018)